CHAPTER 1

INTRODUCTION

1.1 Introduction

Pupillometry, specifically relative afferent pupillary testing (RAPD), is a valuable diagnostic tool used to assess and quantify abnormalities in the pupillary response to light stimuli. Traditionally, the swinging flashlight test has been employed to detect an afferent pupillary defect, also known as a Marcus Gunn pupil. However, pupillometers have emerged as a more advanced and accurate alternative for conducting relative afferent pupillometry (RAPD).

The swinging flashlight test involves comparing the direct and consensual pupillary responses by shining a light alternately in each eye. The examiner observes the pupillary constriction and dilation in response to light, and any asymmetry in the pupillary response suggests the presence of an afferent pupillary defect. While this method can provide qualitative information about the presence or absence of a RAPD, it is subjective and relies heavily on the examiner's interpretation.

Pupillometers, on the other hand, offer objective and quantitative measurements of pupillary responses. These devices utilize infrared light sources and detectors to capture and analyze the pupillary dynamics accurately. By measuring the pupil radius. pupillometers provide precise and reproducible data, enabling a more accurate assessment of RAPD severity.

Pupillometers also offer additional advantages over the swinging flashlight test. They eliminate the potential for examiner bias and variability in interpretation, as the measurements are standardized. Pupillometers can generate numerical values that can be compared and tracked over time.

Furthermore, pupillometers often come equipped with software that enables comprehensive analysis and documentation of pupillary responses. They can generate graphical representations of pupillary dynamics, allowing for easy visualization and comparison of data points. These features are particularly beneficial for research purposes, as they facilitate data analysis, statistical evaluation, and inclusion in scientific publications.

1.2 Aim of the thesis

To develop a novel pupillometer specifically designed for the accurate diagnosis and assessment of Relative Afferent Pupillary Defect (RAPD), also known as the Marcus Gunn pupil. The existing methods for detecting RAPD, such as the swinging flashlight test, are subjective and prone to examiner interpretation, leading to potential diagnostic inaccuracies so, this design and construct a pupillometer that employs advanced technology and precise measurements to detect and quantify RAPD objectively and trained the model to differentiate the classes of eye images as Cataract, Blurry vision, Normal vision from the dataset obtained.

1.3 Objective of thesis

1.3.1 General Objective

The main objective of this thesis is to design and develop a Pupillometer for detection of Relative afferent pupillary defect using deep learning for patients suffering with asymmetry response of pupil to the light stimulus.

1.3.1 Specific Objectives

The specific objectives of the thesis are as follows:

1. Design and develop a pupillometer prototype that incorporates hardware components to give the best pupil response to the light stimulus.
2. Capturing the eye images using the device under the stimulus and under normal light and preparing the data set.

3. Development and implementation of feature extraction algorithms for pupil detection.
4. Classification and training of obtained data set into various classes.
5. Evaluate the sensitivity, specificity, and accuracy of the trained model in detecting the radius of the pupil and its classification.
6. Based on the obtained radius, displaying the RAPD status and classification of eye defects.

1.4 Scope of the thesis

The development of the project is to contribute towards improving the life of RAPD patient in detection at early stage and satisfying the technological needs of medical health care providers. This can be achieved by developing model that gives the best pupil response to the light stimulus with an functional feasibility that would enable them to diagnose RAPD and eye defects at early stage. This work aims to implement a model for RAPD patients and a patient suffering from eye defects.

1.5 Background information

1.5.1 Relative afferent pupillary defect

The pupillary light reflex is a vital physiological response mediated by the autonomic nervous system. It involves the constriction of the pupil in response to light stimulation, which is controlled by the pupillary muscles of the iris. The relative afferent pupillary defect (RAPD), also known as the Marcus Gunn pupil, refers to an abnormality in the pupillary light reflex that indicates asymmetrical visual pathway function between the two eyes.

Traditionally, RAPD has been assessed using subjective clinical methods, most notably the swinging flashlight test. This test involves shining a light alternately between the two eyes and observing the pupillary responses. A relative decrease in pupillary constriction in one eye compared to the other suggests the presence of RAPD. However, the swinging flashlight test is prone to subjective interpretation and variability among examiners, leading to potential diagnostic inaccuracies.

To overcome these limitations, pupillometry has emerged as an objective and quantitative method for assessing RAPD. Pupillometers are specialized devices that utilize advanced

technology, including light sources and software algorithms, to accurately measure and analyze pupillary responses. By quantifying key parameters such as baseline pupil size, pupil radius. pupillometers provide objective and reproducible data for RAPD assessment.

The development of a pupillometer specifically designed for the detection of RAPD holds significant clinical and diagnostic value. It can improve the accuracy and reliability of RAPD diagnosis, aid in the early detection of optic nerve dysfunction and retinal disorders and facilitate monitoring of disease progression and treatment effectiveness.

By incorporating pupillometry into the development of a specialized pupillometer for RAPD detection, this thesis aims to address the limitations of subjective diagnostic methods and contribute to the advancement of objective and accurate assessment of RAPD. The integration of advanced hardware components, software algorithms, and validation studies will enable the creation of a reliable and user-friendly pupillometer that can enhance clinical decision-making, improve patient care, and expand our understanding of pupillary dysfunction in various pathological conditions.

Detection of RAPD can be interrupted by eye defects include cataract, blur vision. Etc. The formation of cataract layer i. e Cortical Opacities due to which the obtaining of radius of pupil will be difficult, so here we divided the eye images into various classes such as cataract, blurry vision, and normal images.

1.5.1.1 Grading of relative afferent pupillary defect

Relative afferent pupillary defect (RAPD), also known as the Marcus Gunn pupil, is graded using the swinging flashlight test. The test involves comparing the pupillary responses of the two eyes when a flashlight is alternately directed between them. The degree of RAPD can be assessed and graded based on the differences observed in pupillary constriction. Here is a commonly used grading scale for RAPD:

Grading	Pupil response
0	No RAPD or normal pupillary response.
+1	Mild RAPD: There is a subtle decrease in pupillary

	constriction in the affected eye.
+2	Moderate RAPD: There is a noticeable decrease in pupillary constriction in the affected eye.
+3	Marked RAPD: There is a significant decrease in pupillary constriction in the affected eye.
+4	Severe RAPD: The affected eye shows minimal or no pupillary constriction in response to light.

Explanation of RAPD Grading:

1. Grade 0: A grade of 0 indicates no RAPD, meaning both eyes exhibit normal and equal pupillary responses. The pupils constrict symmetrically when exposed to light, suggesting no significant asymmetry in the afferent pathways.
2. Grade +1: A grade of +1 indicates a mild RAPD. The affected eye demonstrates a subtle decrease in pupillary constriction compared to the unaffected eye. The difference may be subtle and require close observation to detect.
3. Grade +2: A grade of +2 suggests a moderate RAPD. The affected eye shows a noticeable decrease in pupillary constriction compared to the unaffected eye. The difference is more apparent and easily observed during the swinging flashlight test.
4. Grade +3: A grade of +3 represents a marked RAPD. The affected eye exhibits a significant decrease in pupillary constriction compared to the unaffected eye. The difference is pronounced and easily observed during pupillary testing.
5. Grade +4: A grade of +4 indicates a severe RAPD. The affected eye shows minimal or no pupillary constriction in response to light, regardless of the intensity. The lack of pupillary response suggests a substantial impairment in the afferent pathway of the affected eye.

1.5.2 Cataract

Cataract is a common eye condition characterized by the clouding or opacity of the eye's natural lens, which is located behind the iris and is responsible for focusing light onto the retina. The clouding of the lens occurs due to the build-up of proteins and other substances, leading to a loss of transparency and visual impairment.

In the context of relative afferent pupillary defect (RAPD), cataract can potentially interfere with the accurate measurement of pupillary responses. RAPD is an abnormal pupillary response seen in cases where there is a significant difference in the afferent signals (information coming from the retina) between the two eyes. It is often associated with optic nerve dysfunction or asymmetrical retinal input.

When cataracts are present, the clouded lens can cause light to scatter and reduce the amount of light reaching the retina. This scattering effect can result in a decreased overall amount of light reaching the affected eye compared to the healthy eye. As a result, the pupillary response in the eye with cataract may be reduced or altered, leading to an apparent difference in pupillary response between the two eyes during pupillary testing.

During the measurement of RAPD, a swinging flashlight test is commonly performed. In this test, a light source is alternately directed between the two eyes, and the pupillary responses are observed. The examiner compares the relative changes in pupillary size and constriction between the two eyes.

In the presence of cataract, the clouded lens may impede the accurate assessment of pupillary responses. The scattered light and reduced transmission through the cataractous lens can lead to a less pronounced pupillary constriction or delayed pupillary response in the affected eye. This can create a false appearance of relative afferent pupillary defect, suggesting a greater impairment of the affected eye's pupillary response compared to the healthy eye.

It is essential for clinicians to be aware of the potential impact of cataracts on pupillary testing and interpretation of RAPD. The examiner should consider the presence of cataracts as a possible confounding factor and take it into account when evaluating pupillary responses. In some cases, additional diagnostic methods, such as imaging studies or consideration of other clinical findings, may be necessary to confirm the presence and extent of RAPD in individuals with cataracts.

1.5.3 Blurred vision

Blurred vision refers to a visual impairment characterized by a lack of sharpness or clarity in one's vision. It can occur in various eye conditions, including cataracts, refractive errors (such as near-sightedness or farsightedness), and certain retinal disorders.

In the context of relative afferent pupillary defect (RAPD), blurred vision can impact the measurement and interpretation of pupillary responses. RAPD is an abnormal pupillary response that occurs when there is an asymmetrical function or input between the two eyes' afferent pathways, typically involving the optic nerve or retina.

When an individual has blurred vision, it means that their visual acuity is reduced, and objects appear less defined or fuzzy. This reduction in visual acuity can affect the accuracy of pupillary testing and the assessment of RAPD. Here's how blurred vision can lead to interruptions in measuring relative pupillary defect:

Pupillary Constriction: Blurred vision can affect the ability to accurately assess pupillary constriction, which is a critical parameter in evaluating RAPD. When vision is blurred, the examiner may have difficulty precisely observing the extent of pupillary constriction or the differences in constriction between the two eyes. This can potentially result in an underestimation or overestimation of pupillary responses, leading to an inaccurate assessment of RAPD.

Perception of Light Intensity: Blurred vision can alter the perception of light intensity, making it challenging to accurately compare the pupillary responses between the two eyes. The individual's subjective experience of light intensity may differ due to the blurring effect, which can introduce inconsistencies in the evaluation of RAPD.

Interpretation of Visual Field Defects: Blurred vision can also be associated with visual field defects, where there are areas of reduced or absent vision in the visual field. Visual field defects can influence the pupillary responses during RAPD testing. The presence of visual field defects, in conjunction with blurred vision, can complicate the identification and assessment of RAPD, as the underlying cause of the relative defect may be difficult to differentiate solely based on pupillary responses.

CHAPTER 2

LITERATURE REVIEW

2.1 Review of work done by various authors on pupils and RAPD

The pupillary light reflex was initially used in medicine by Galen in the second century A.D. While the patient was looking out the window, he would conceal and then uncover each eye in turn. The good eye's pupil contracted when exposed, whereas the damaged eye's pupil dilated. It is a quick and easy examination that doesn't require any special equipment, but because it is impractical (open windows are no longer available to look through), it has gradually lost favour in clinical settings. Galen and his contemporaries considered pupillary reflexes to be a reliable indicator of the presence of vision. Although there is no direct pupillary response in unilateral blindness, Graefe asserted the same in 1855.

Despite the absence of a direct pupillary response, when the other eye is activated, the pupil will respond. In 1846, Gerold made a comment about the concomitant dilating of one pupil when the other eye was covered in his book on black cataracts. Hirschberg first described a case of a woman who experienced sudden, severe vision loss with no PLR on that side and linked PLR attenuation to optic nerve illness. In a case of retrobulbar neuritis that he presented in 1901, Baquis highlighted the following: (a) absence of the direct light reaction in the affected eye; (b) persistence of the consensual reaction in the affected eye when the healthy eye was stimulated; (c) absence of anisocoria; and (d) consensual dilating of the pupil of the affected eye.

A retrobulbar neuritis-dimmed eye had a poor pupillary response to light, whereas an eye with functional amblyopia had a good pupillary constriction to light following repeated light stimulation, according to Marcus Gunn in 1904. To define such an afferent pupillary deficiency, Kirshenbaum popularised this pupillary sign and named it after Marcus Gunn forty years later.

In 1959, Levatin made a wise and helpful recommendation. He replaced the alternate cover with an alternate torch. Thompson later formalised it. The pupils of both eyes constrict in cases of unilateral or asymmetric optic nerve illness when the torch is presented in the healthy eye, but they dilate when the torch is shown in the bad eye.

Clinical testing can identify relative afferent pupil defects (RAPD) as tiny as 3 dB, and the sensitivity can be increased by putting a 3-dB neutral density filter (NDF) in front of the suspected problematic eye to increase the inter-eye pupillomotor drive to a detectable level. By using NDF, crossed polarising filters, or Bagolini filters of increasing value in front of the good eye until the RAPD is neutralised, the degree of RAPD can be accurately measured. Bell introduced the 3-second pause technique to the test in order to standardise it. Bell claimed that there was a strong connection in all RAPD grades between different residents and provided comparable values for Neutral Density Filters for each grade.

The swinging flashlight test has become the most common clinical test in clinics; it requires only one pupil and is easily quantifiable and much more sensitive.

The test is deceptively simple, however, and requires considerable practice to perform reliably as well as care in its interpretation; inexperienced clinicians may induce an RAPD by unequal retinal bleaching or by off-axis stimulation in patients with strabismus. Patients must not focus on the flashlight since accommodative miosis will be greater when the light is shown in the better eye.

Normal subjects may show RAPD up to 3 dB due to natural asymmetry in the pupillomotor drive from the two eyes. Furthermore, anisocoria will generate RAPDsof approximately 1 dB for each 1 mm of anisocoria by limiting the amount of light entering the eye with the smaller pupil. Media opacities may induce an RAPD in the fellow eye by increasing the scatter and thus the pupillomotor ‘effectiveness’ of the light stimulus.

Stern in 1944 first published a new method of testing pupillary light reflex using the slit lamp light source as stimulus and a stopwatch. In this procedure, a small beam of slit lamp light is directed into one eye and with the subsequent constriction of the pupil, turns off the stimulus, leading to pupil dilation that turns the light stimulus back on and producing endless cycling. Dysfunction anywhere along the PLR pathway is expected to reduce the frequency of these oscillations and therefore prolong their period. Thompson and Miller in 1978 improved this technique and called it pupil cycle time. They timed 30 oscillations using a stopwatch and repeated these five times to give an average estimate. Using this approach, PCT measurements have since been made in patients with a wide variety of optic neuropathies (optic neuritis, compressive optic neuropathy, glaucoma, atrophic papilledema, traumatic optic neuropathy, and ischaemic optic neuropathy). There are many drawbacks for this test; the test duration being 5 min long made it difficult for the patient and clinician, the background conditions and the intensity are not standardized, not suitable to test severe diseases as it is impossible to induce pupillary oscillations. As the test results

are influenced by the disease present anywhere else in PLR pathway, it is not a valid test to perform in patients with autonomic dysfunction and iris abnormalities. Compared to Swinging flashlight test PCT measurements are found to be less sensitive in detecting mild abnormalities.

Wilhelm Helmut et al., did a study to see prevalence of RAPD in normal subjects and found that in normal population an RAPD of 0.3 log units (the threshold that is detectable using swinging flashlight test when performed correctly) is present in fewer than 2% population, and an RAPD of >0.39 log units was not found.

2.2 Brief review of the work done by various authors on the use of Pupilometers in determining pupil size, parameters, and their use in Detecting RAPD.

Radzius, Aleksandras, et al. worked on Infrared pupillometer that measures the pupil radius and the change in pupil radius after its response to a light stimulus and the values obtained were comparable to a photographic measurement. Lada Kalaboukhova, Vanja Fridhammar, and Bertil Lindblom studied on patients with Optic Atrophy due to Unilateral Open-angle glaucoma with an aim to develop a new technique to analyse RAPD and to find the optimum stimulus parameters for RAPD detection in those patients. They used custom built pupillometer and different sets of stimulus-pause combinations were studied (1s-0.5s, 0.5s-1s, 1s-1s, 1s-1.5s, and

1.5s-1.5s) and their study results showed that the combination of a stimulus duration of 0.5 s and a pause duration of 1 s at a light intensity of 1000 cd/m2 was best suited for the detection of glaucoma.

The relative afferent pupillary defect was shown quantitatively in an eye

Contralateral to dense unilateral cataract, recorded using a binocular infrared video Pupillography. The difference between contraction amplitudes (which was defined as the difference between maximal and minimal radiuss of the pupil of an eye) was larger when compared between right eye stimulation and left eye stimulation before the surgery with constrictions being higher when the cataractous eye was stimulated. This difference in contraction amplitude disappeared after surgery in the cataractous eye.

Pupillary responses were examined quantitatively in three patients with unilateral extensive myelinated nerve fibres and amblyopia using binocular infrared Video pupillographic device (Vision module; Newopto, Kawasaki, Japan) in a darkened room by presenting

stimuli with white light-emitting diodes to the right and left eyes alternatively. They noticed that there was percent reduction in pupil contraction amplitude (the sum of both pupils) during the stimulation of the affected eye. The average of constriction amplitudes (constriction amplitude for each light reflex was defined as the difference between maximum and minimum radiuss) for the four right eye stimulations was then compared with the average of the four left eye stimulations.

Cohen, Liza M., et al., worked on a Novel and Computerized pupillometer. The pupil responses obtained in RAPD patients are correlated with the RAPD's stimulated by presenting different illumination intensity (LUX) to both eyes and clinician determined RAPD are correlated with the device calculated RAPD. They found a significant correlation in both cases. They determined the eye with RAPD, and the degree of it is calculated by the ratio of percentage change in the constriction amplitude to the right eye and left eye stimulation. Based on study results they concluded that the device had high sensitivity and specificity. As per literature, this is the only available device which can actually detect the eye with RAPD and the degree of RAPD.

Volpe, Nicholas J., et al., say that the pupillometer device distinguishes between healthy volunteers and patients with RAPD greater than 0.9 log units of neutral density filter reducing its sensitivity. In this study, there is the significant statistical difference between normal and RAPD patients and significant correlation between patients with true APD's and subjects with stimulated RAPD's using neutral density filters.

Cox, Terry A worked with a binocular television pupillometer, recording the pupillary responses of normal subjects after stimulating RAPD using neutral density filters to dim the light in front of one eye while performing the swinging flashlight test.

They aimed to determine the best indicator of RAPD by comparing contraction amplitude, minimum size, final size, and re-dilatation amplitude. Their study concluded that the contraction amplitude is the best indicator.

Volpe, Nicholas J et al., again worked on a computerized pupillometer device.

They compared the NDF strength required to neutralize the RAPD of the patient for whom the device also calculates the absolute inter-eye difference, and they found a significant correlation between both findings. But there is also an inter-eye difference found by the device in normal subjects, which questions the device capability in distinguishing normal from abnormal.

A study carried using a pupillometer to determine whether there is any difference in constriction amplitude between both the eyes in 10 patients with various degrees of

amblyopia showed that only a small proportion of amblyopes actually show difference in constriction amplitude. Dara Lankaranian compared the sensitivity and specificity of detecting RAPD using routine Swinging flashlight test method and
Pupillography method on patients having glaucoma and concluded that the
Pupillography with a magnified view of pupils helps in better detection of RAPD.
A study, done by Benson, M. T., et al. showed a positive scope for the further development of the device using which the mean difference of pupillary responses between right and left eye were calculated. They found a significant difference between the mean differences of normal subjects and patients with APD. The mean difference between right and left eyes was 8.84 ms for normal and 78.6 for patients with APD. Shwe-Tin calibrated pupillometer output with the neutral density filters of attenuation: 0.0, 0.3, 0.6, and 0.9 log units and tested it on healthy volunteers by stimulating RAPD with NDF's of the same attenuation. The sensitivity and specificity of the device detecting stimulated RAPD with NDF was high. Thus, they gave future directions for using this device to detect RAPD in actual patients.

2.3 Existing GAP and Proposing a Novel Device

Although there have been multiple studies describing many pupilometers and their use in detecting RAPD throughout many decades, till date there is no pupillometer that got incorporated into clinical practice and achieved widespread use.
This could be because of the lack of availability of an established pupillometer that is accepted and believed by clinicians which can replace a traditional swinging light test performed by a well-experienced doctor in detecting the RAPD. RAPD designed by Konan Medical a US based company, is the only pupillomotor device which determines the pupil function and gives quantitative score of RAPD.
Therefore, we are proposing a Novel device to standardize this test using a custom designed hardware and a software routine. Initial prototype of the device was designed by Team Innovation, Srujana Innovation Centre, LVPEI.

CHAPTER 3

ANATOMY AND PHYSIOLOGY

3.1 Human eye

The eye is one of the most intricate, crucial, and unique. They are possibly the most priceless asset we have, and they aid in how we interpret the world. Our daily lives depend heavily on our eyes, and good vision is essential.

Improves the quality of life around the world.

The human visual system consists of a complicated network of structures, each of which serves a particular function. It consists of the following three jackets or tunics:

1) The cornea and the sclera's outer layers of connective tissue

2) The middle-vascularized layer of the uvea, which is made up of the choroid, ciliary body, and iris.

3) The retina's inner neural layer.

The conjunctiva, eyelids, brows, secretory system, and drainage system are all parts of the ocular adnexa. The anterior chamber, posterior chamber, and vitreous chamber are the three spaces that make up this globe. There is a crystalline lens in the region of the posterior chamber.

Conjunctiva: The transparent mucous membrane that lines the inside of the eyelids is called the conjunctiva.

The conjunctiva is divided into the palpebral conjunctiva, which covers the eyelids, the forniceal conjunctiva, and the bulbar conjunctiva as far as the limbus.

At the limbus, the conjunctiva covers the anterior sclera and is continuous with the corneal epithelium.

Cornea: The primary refracting element of the eye is the cornea. It has a translucent, avascular makeup. The cornea is made up of five layers: the epithelium, Bowman's layer, stroma, Descemet's membrane, and endothelium. These layers are arranged from anterior to posterior. Tear film covers the cornea's anterior surface, while the posterior surface borders the aqueous-filled anterior chamber. The conjunctiva and sclera are continuous, with the cornea at its edge.

The cornea serves two main purposes: both to transmit light and to refract it.

Light rays can pass through the clear cornea into the globe and are helped to focus on the retina by refraction.

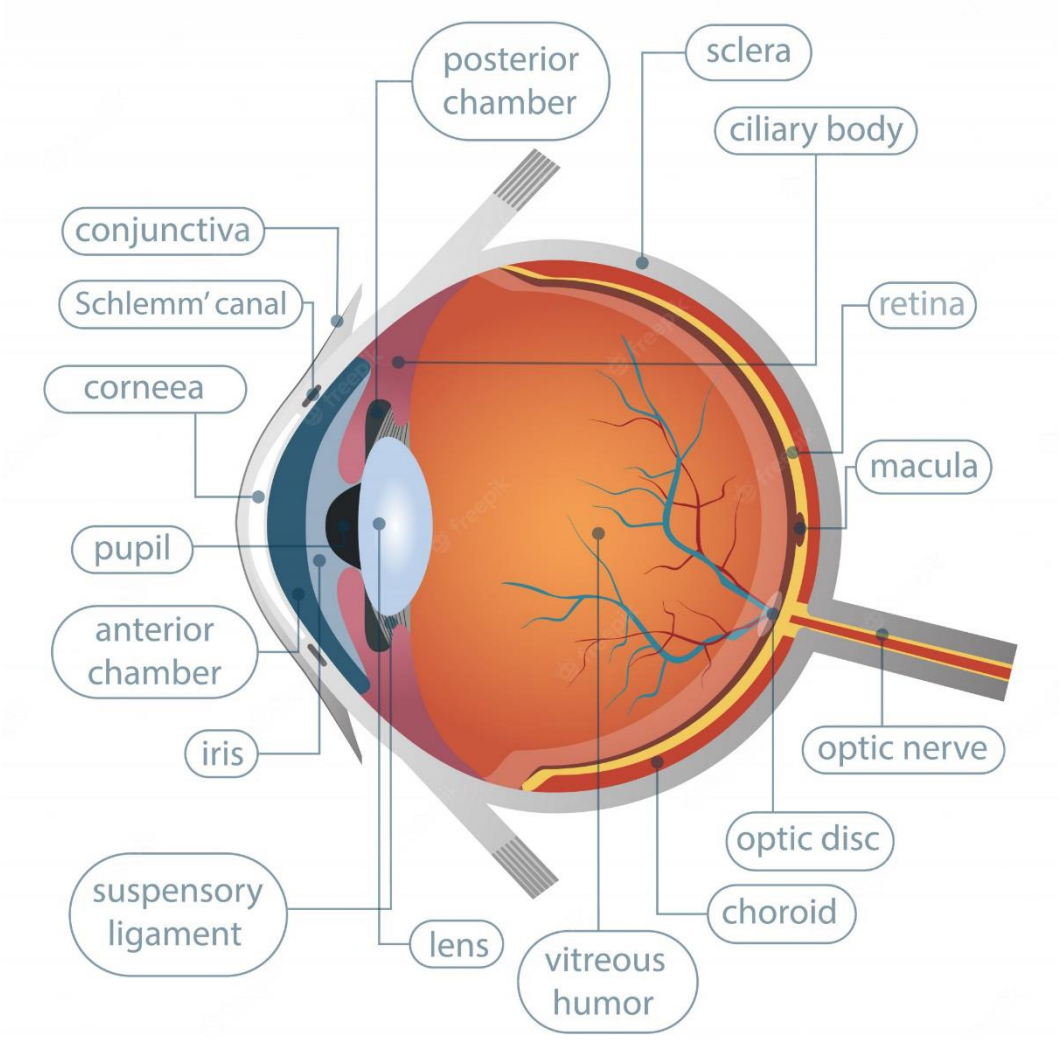

Figure 3.1 Anatomy of Visual System

Sclera: The conjunctiva, which is transparent, covers the opaque white of the eye called the sclera. It makes up the back half (or five-sixths) of the globe's connective tissue coat. The sclera serves as an attachment for the extraocular muscle insertions and preserves the shape of the eyeball by providing resistance to internal and external stresses. The limbus is the area where the sclera and conjunctiva transition from the cornea. The central, vascular layer of the eye is called the uvea. Iris, ciliary body, and choroid make up its structure.

Uvea: The central, vascular layer of the eye is called the uvea. Iris, ciliary body, and choroid make up its structure.

Iris: The iris is a small, circular, pigmented structure that is anterior to the pupil.

lens: It divides the space between the cornea and lens into the anterior and posterior chambers while suspended in the aqueous humour there.
Pupil refers to the iris's centre opening. The central pupillary zone and the peripheral ciliary zone are located on the anterior surface of the iris. A round ridge called the collarette, which is located about 2 mm from the pupil, serves as the boundary. The sphincter pupillae and dilator pupillae are the muscles that make up the stroma of the iris.

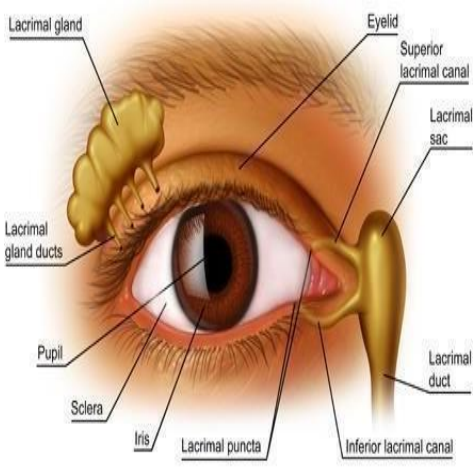

Figure 3.2 Anatomy of eye Ventral view muscles

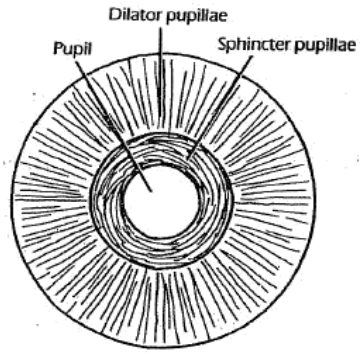

Figure 3.3 Anatomy of Iris

Meiosis (contraction): The sphincter muscle, or miosis, is a ring-shaped muscle that surrounds the pupil. The pupil is constricted by the sphincter pupillae during accommodation and in strong light. The muscle is innervated by the parasympathetic system.

The muscle fibres of the dilator are oriented radially during mydriasis (dilation). In low-light conditions and when feeling anxious or excited, the pupil dilates due to the dilator pupillae. There is sympathetic innervation in the dilator. The pupil's exposure to light is controlled by the iris, which functions as a diaphragm. The retina's lighting is controlled by pupil size.

Mydriasis (dilation): The muscle fibres of the dilator are oriented radially during mydriasis (dilation). In low-light conditions and when feeling anxious or excited, the pupil dilates due to the dilator pupillae. There is sympathetic innervation in the dilator. The pupil's exposure to light is controlled by the iris, which functions as a diaphragm. The retina's lighting is controlled by pupil size.

Ciliary body: The iris's periphery continues posteriorly into the choroid and is continuous with the ciliary body. The ciliary epithelium, ciliary stroma, and ciliary muscle make up the ciliary body. Pars refers to the ciliary body's anterior surface.

The posterior surface of the plicata, which gives birth to the ciliary processes and through which the zonule fibres that attach the lens pass, is pars plana. Aqueous humour is produced and secreted by the ciliary processes of the ciliary body. It is concerned with how the lens and its musculature are suspended from the ciliary muscle, which can lead to accommodation and have an impact on aqueous outflow.

Choroid: The inner surface of the sclera is lined with a thin, supple, and brown covering called the choroid.

It runs from the optic nerve's posterior end to the ciliary body's anterior end and is exceedingly vascular. It is situated between the retina and the sclera.

The choroid's main job is to supply the retina's outer layers with blood via its blood veins. It transports several blood vessels to the eye's anterior. Reflection is avoided because the pigment

cells of the choroid absorb extra light that enters the retina.

Retina: The retina, a neuronal layer that lies between the choroid and the vitreous, is the eye's innermost layer. It is contiguous with the ciliary body's epithelial layers. The macula, the region at the posterior pole used for the finest sharpness and colour, is part of its vision.

It extends from the optic disc's rounded border, where the nerve fibres leave the eye and travel to the brain as the common optic nerve. The disc serves as the physiologic blind spot since it lacks photoreceptor cells, so light impinging on the disc has no effect. The retina is made up of an inner neurosensory layer and an outer pigmented layer.

The neural retina seems to be a thin, translucent membrane, despite the fact that it is made up of millions of cell bodies and their processes.

The retina is where light energy is converted into a neuronal signal. The visual pathway, which is how visual information from the environment travels to the brain to be interpreted, contains the first three cells (photoreceptor, bipolar, and ganglion) along that pathway. Through the process of phototransduction, photoreceptor cells convert light photons into neural signals that are subsequently transferred to bipolar cells, which in turn synapse with ganglion cells to convey the signal from the eye. Before the signal exits the eye, other retinal cells, including horizontal cells, amacrine cells, and interplexiform neurons, modify and integrate it.

Lens: Behind the iris and pupil and in front of the vitreous body is the clear, avascular, biconvex lens. By using zonular fibres, the lens is held in place by the ciliary body around it.

It helps concentrate light on the retina. It is flexible, and ciliary muscle contraction can modify the curvature of the lens, increasing the dioptric power of the eye through a process known as accommodation that enables close objects to be focused on the retina.

Anterior chamber: From the posterior surface of the cornea to the anterior surface of the iris is the anterior chamber.

Posterior chamber: The posterior chamber is located between the iris and the retina.

Aqueous humour: Aqueous humour is created by the ciliary body and is present in both the anterior and posterior chambers, which are connected by the pupil. The surrounding structures, especially the cornea and lens, are nourished by the aqueous humour.

Vitreous humour: The vitreous humour, the largest space, is bordered in front by the lens and is located next to the inner retinal layer. The vitreous humour, a fluid-like material, is present in this chamber.

The secretory system of the eye is made up of the primary lacrimal gland, auxiliary lacrimal glands, meibomian and Zeis glands, and conjunctival goblet cells. They assist in maintaining ocular moisture by secreting various tear film constituents. The puncta, canaliculi, lacrimal sac, and nasolacrimal drainage system, as well as the nasolacrimal duct, which drains around 75% of tear fluid into the nasal cavity.

Binocular vision is made possible by the coordination of the muscles in both eyes, which are extra ocular muscles linked to the outer layer of the eye. The eyelids' muscles enable them to open and close as well as elevate and depress the lids when they are open, mimicking the movement of the globe caused by EOM. The eye and its surrounding tissues and structures get sensory and motor innervations from a complex network of nerves, as well as nutrition from a network of blood vessels.

3.2 Visual System and the way it responds to light

Light-based information from the environment is taken in by the visual system. The components that convert light rays into neural signals are housed in the eye. The light beams from infinity strike the eye, bounce off the cornea's primary refracting

surface, and enter the eyeball's anterior chamber. In bright and low-light circumstances, the pupils contract and dilate to control the amount of light that enters the eye. The crystalline lens, the second refracting medium in the eye, is where the light rays are refracted before falling on the retina.

The retina is where light energy is converted into a neuronal signal. The visual pathway, which is how visual information from the environment travels to the brain to be interpreted, contains the first three cells (photoreceptor, bipolar, and ganglion) along that pathway. Visual pigment molecules are found in photoreceptor cells, which use the process of photo transduction (a biochemical change) to convert photons of light into neural signals. These signals are then transferred to bipolar cells, which synapse with ganglion cells, which transmit the signal from the eye. Before the signal exits the eye, other retinal cells, including horizontal cells, amacrine cells, and interplexiform neurons, modify and integrate it. Through the filaments of the second cranial nerve, the optic nerve, this is further sent to the brain.

Along with transferring visual information like brightness perception, colour perception, and contrast sensitivity through visual fibres, the optic nerve also conducts impulses through its nerve fibres that are responsible for one of the key neurological reflexes referred to as the light reflex, occurs through afferent fibres known as pupillary fibres via an afferent neural route and causes both pupils to contract when light is shone into either eye. The afferent pathway in a neurological system denotes the signal transmission from a sensory organ to the brain (from the eye to the midbrain).

A precise vision of the surroundings is made possible by the central nervous system's highly developed pathway, through which the neural signal carrying visual information travels. Numerous judgements and actions are influenced by this information, which is assessed through a process known as visual perception. Each structure's arrangement allows it to fulfil its intended purpose.

3.3 Anatomy of pupillary pathway

An important tool for detecting clinical issues with pupillary symptoms is an understanding of the pupillary light pathway. Four neurons serve as sub-receptors for the retinal photoreceptors, which mediate the light reflex. Light strikes the retina, stimulating the ganglion cells that are photosensitive and contain melanopsin.

3.3.1 Afferent Pupillary pathway (Sensory)

1. First (sensory) links both pretectal nuclei in the midbrain with each retina at the superior colliculi, or level. Fibres conducting impulses from the nasal retina decussate in the chiasm and pass up the opposing optic nerve tract to finish at the pretectal nucleus on the opposite (contralateral) side. Uncrossed fibres (ipsilateral optic tract) that end in the ipsilateral (same side) pretectal nucleus carry impulses that originate in the temporal retina.
2. The second (internuncial) link links both Edinger-Westphal nuclei to each pre-tectal nucleus. As a result, unilateral light stimulation causes symmetrical and bilateral pupillary constriction.

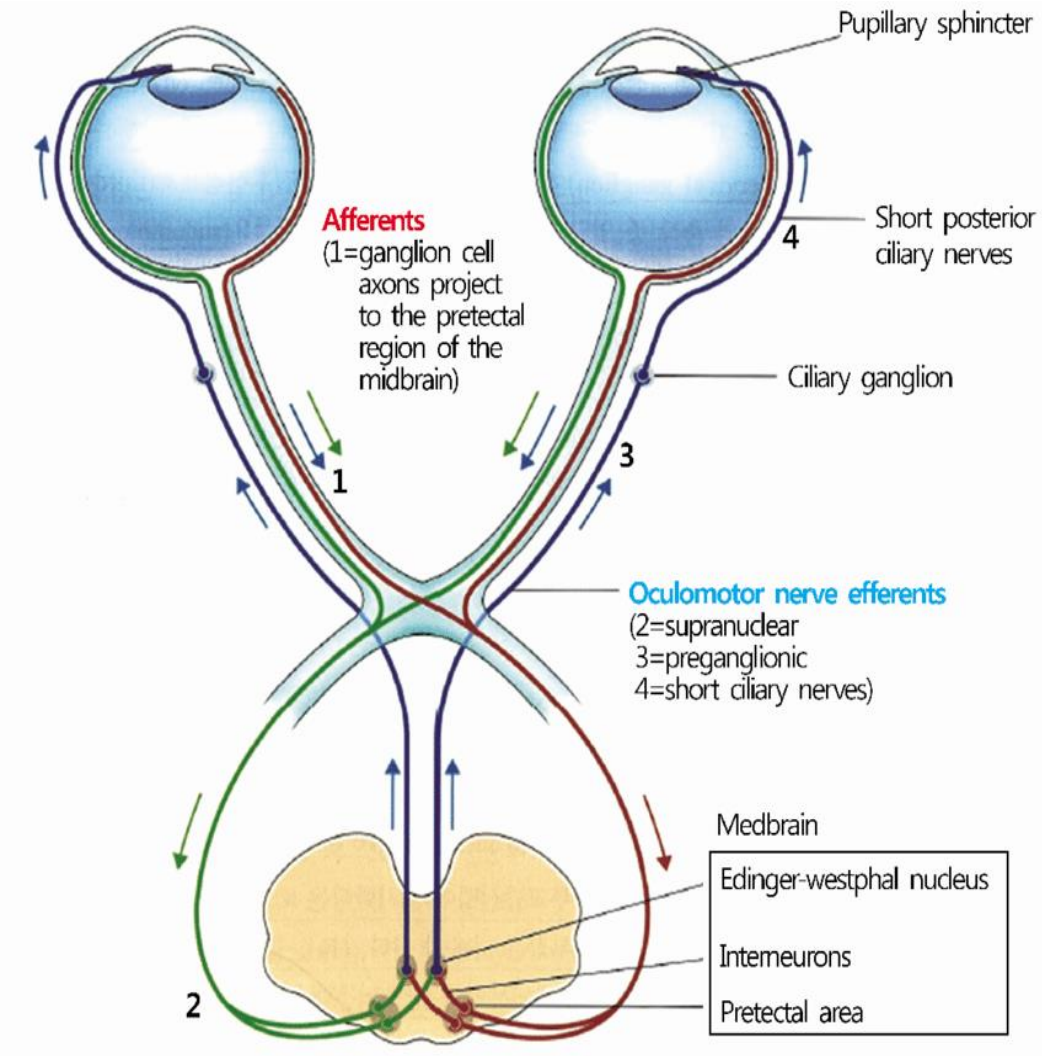

Figure 3.4 Anatomy of Afferent pupillary pathway

3.3.2 Efferent Pupillary Pathway - Parasympathetic (Constriction)

1. The Edinger-Westphal nucleus is connected to the ciliary ganglion by the third (preganglionic motor) fibre. The parasympathetic fibres enter the interior division of the oculomotor nerve and travel there to the ciliary ganglion.
2. The fourth (postganglionic motor) enters the short ciliary nerves to innervate the sphincter pupillae after leaving the ciliary ganglion. Just behind the globe, within the muscular cone, is where the ciliary ganglion is situated.

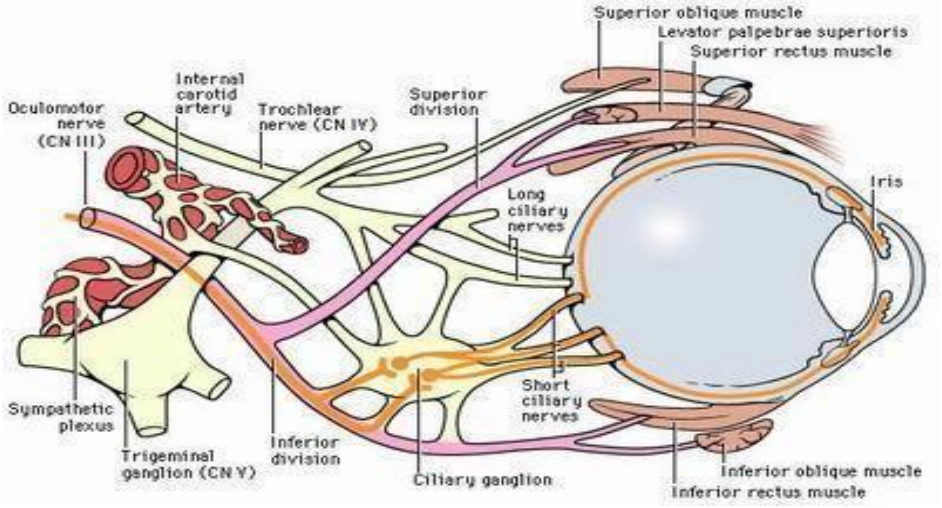

Figure 3.5 Anatomy of Efferent pupillary pathway (Constriction)

3.3.3 Efferent Pupillary Pathway - Sympathetic (Dilation)

1. Begins in the hypothalamus and descends to the spinal cords C8-T2 region (Budge's ciliospinal centre)
2. It leaves the spinal cord and forms synapses in the superior cervical ganglion.
3. Postganglionic fibres enter the superior orbital fissure after travelling down the internal carotid artery.
4. Join the trigeminal nerve's ophthalmic division (cranial nerve V). 5. The ciliary ganglion is traversed by nasal ciliary nerves without synapsing. 6. Long ciliary nerves pass through the radial dilator muscle before terminating.

Direct and Consensual light reflex:

In normal eyes, unilateral light projection produces bilateral pupil constriction.

- Pupil constriction in the eye where light is projected – Direct reflex

- Pupil constriction in the other eye – Consensual reflex

Reasons for consensual reflex:

- Decussation of nasal fibres
- Bilateral projection from Pretectal nucleus to both Edinger-Westphal nuclei

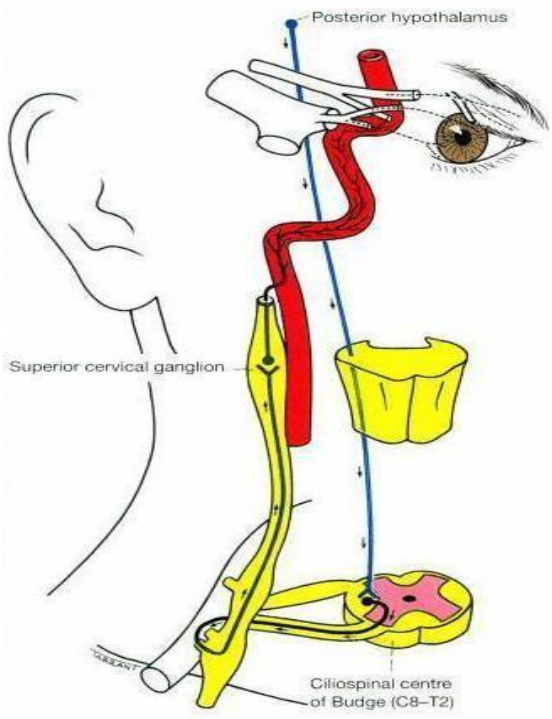

Figure 3.6 Anatomy of Efferent pupillary pathway (Dilation)

3.4 Pupil Evaluation

A routine pupillary examination should look for the following:

(i) The size of the pupils in mm, pupil size is expressed. It is important to determine whether the students are equal.

Pupillary reaction.

(ii) In healthy pupils, both pupils should respond quickly, simultaneously, and equally when light is shone into either eye. Any abnormalities in the eye are indicated by a sluggish response.

(iii). Pupillary shape Normal eyes have round pupils; thus, any deviation, such as ones that are oval, sector, or irregular, indicates problems.

(iv) Peripheral reflexes Direct and consensual light responses are tested using the swinging flashlight method.

Light-near dissociation is tested for in the near reflex. The near reflex is often only examined in the absence of the light reflex.

It is recorded as PERRLA (Pupils Equally Reactive to Light and Accommodation) if the pupils are entirely normal.

Anisocoria is the medical name for when the pupils are not of the same size. Physiological anisocoria is a little discrepancy in pupil size that affects about 20% of healthy individuals. The discrepancy between the pupils in this condition is typically less than 1 mm, which is completely innocuous. If the discrepancy is greater than 1mm, anisocoria may be a sign of more significant medical issues.

3.5 Swinging Flashlight Test (SFT)

As the name says it all, a flashlight is swung alternately between both eyes and the pupillary responses are observed relative to each other.

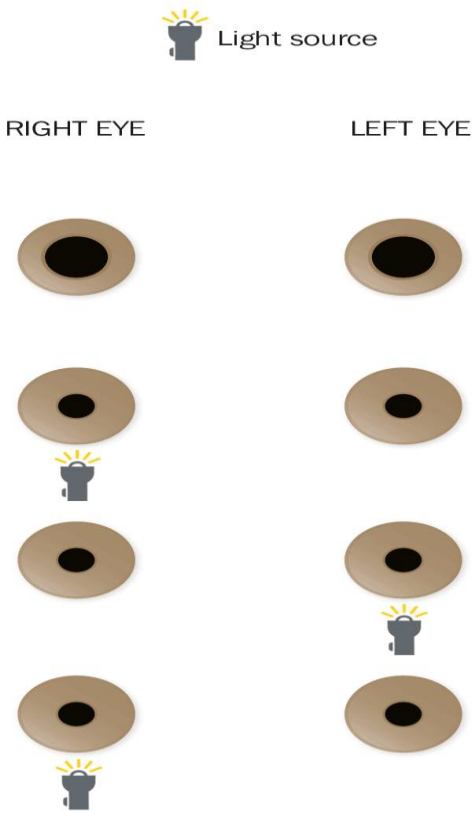

Figure 3.7 Swinging flashlight test

3.5.1 Normal pupillary light reflex

Normal students both eyes' pupils contract equally when light is shined into one of them, and then they both begin to relax a little. When the light is turned off, they expand once more. Both pupils remain constricted when the light is swiftly switched between them (during the pupillary constriction). When light is supplied to both eyes, the pupils of both eyes slightly relax if the length of time the light is present in front of each eye exceeds the mean pupillary constriction time of those pupils.

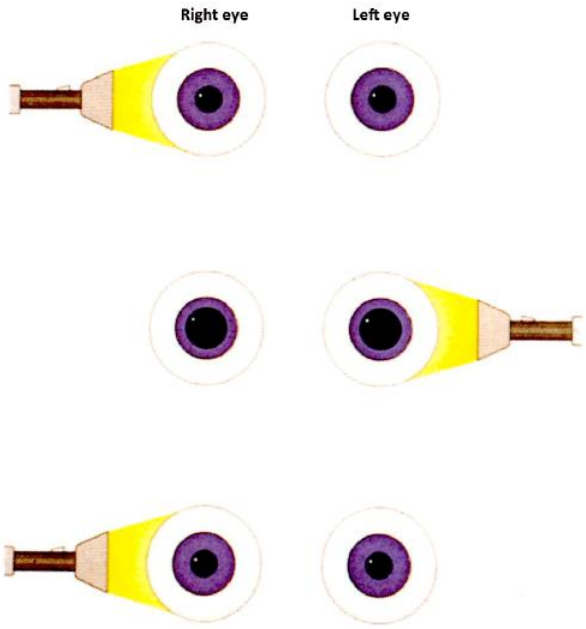

Figure 3.8 Swinging flashlight test showing normal pupillary reflex

Characteristics should be the same in both eyes. Both pupils show similar responses when light is projected either to the right eye or left eye.

3.6 Relative Afferent Pupillary Defect (RAPD) or Marcus Gunn Pupil

Relative Afferent Pupillary Defect (RAPD) results from any ocular illness that causes the normal afferent route of the pupil to be disrupted.
The pupils react quickly to stimulation of the healthy eye and slowly to stimulation of the unhealthy eye. The paradoxical dilation of both pupils in a sick eye when light is present is known as RAPD.

3.6.2 Causes of RAPD

RAPD is primarily seen in unilateral or bilateral, asymmetrical Optic nerve diseases And in Retinal diseases if severe.

Optic Nerve disorders:

• Unilateral Optic Neuropathies: Optic Neuritis, Ischemic Optic Neuropathy, Glaucoma, Traumatic Optic Neuropathy, Optic Nerve tumour

• Orbital disease: Compressive damage to the optic nerve from thyroid related Orbitopathy, Compression from enlarged extra ocular muscles in the orbit, Orbital tumours, Vascular malformations

• Radiation optic nerve damage, Miscellaneous Optic Neuropathies (such as Leber's Optic Neuropathy (usually eventually bilateral) and other inheritable optic Neuropathies), Optic Nerve infections or inflammations, Optic Atrophy – status-post Papilledema, Surgical damage to the optic nerve.

Retinal Causes of a RAPD:

• Ischemic retinal disease: Ischemic central retinal vein occlusion, central retinal artery occlusion, severe ischemic branch retinal or arterial occlusions, severe ischemic Diabetic or sickle-cell retinopathy.

• Ischemic ocular disease: Ocular ischemic syndrome

• Retinal detachment, severe macular degeneration, intraocular tumour (Retinal and Choroidal tumours including melanoma, Retinoblastoma, and metastatic lesion, Retinal infection (Cytomegalovirus, herpes simplex, and other causes of retinitis)

CHAPTER 4

METHODOLOGY

4.1 Design of Prototype

4.1.1 Design Overview

The design of the pupilometer device records the constriction of the pupil of eye when light falls on it. The device is adjusted correctly so that the pupils of both eyes are visible correctly in the window.

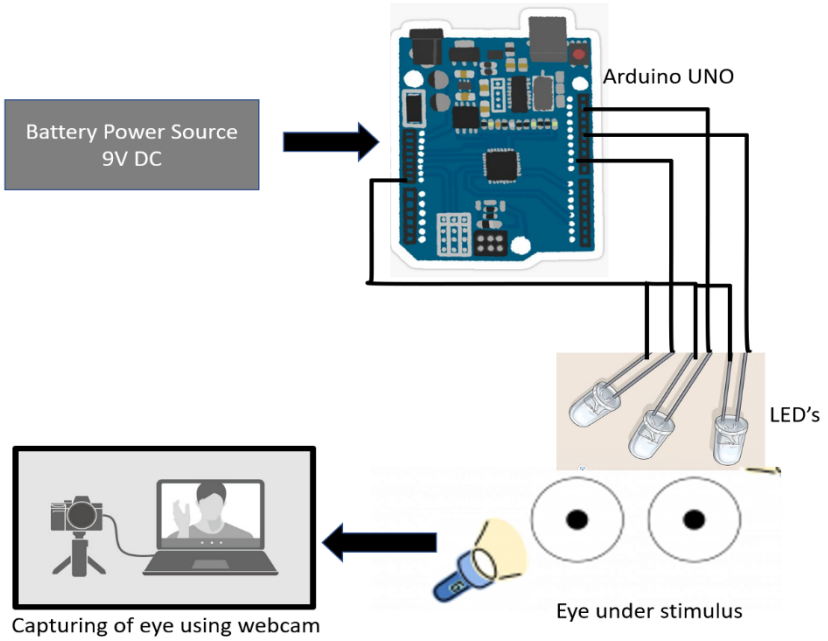

Figure 4.1 Conceptual block diagram of the proposed device

The stimulus alternates between both eyes by lasting in front of each eye for five seconds and a rapid alternation with a gap of three seconds between each stimulus pair. The cameras present inside the device records a live video of pupil of each eye when they are reacting to light stimulus. Once the photographs of eye are taken automatically the further image processing is done and the diameter of the pupil is compared between the eye and displays RAPD status. Recording of video and taking photographs are done by the visual studio open cv and the further process was done by the visual studio python programming.

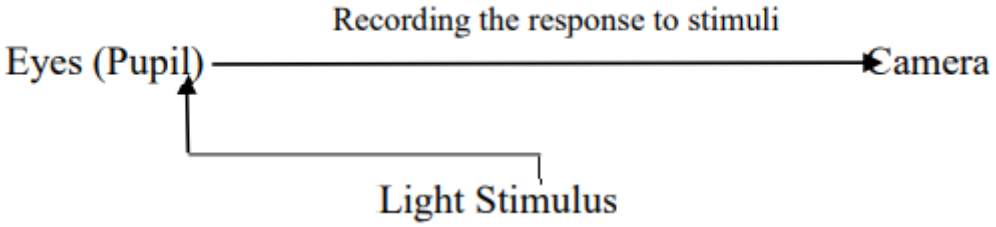

Figure 4.2 concept of the device

4.1.2 Hardware Platform

The components of Pupillometer device are:

Hardware Components:

1. Webcam
2. Arduino UNO
3. White LED's
4. Power bank

4.1.2.1 Webcam

A USB webcam is a camera that connects to a computer, usually through plugging it in to a USB port on the machine. The video is fed to the computer where a software application lets you view the pictures and transfer them to the Internet. This is a Full HD USB camera that enables high-quality video collaboration through laptops, computers and more. This webcam supports 1080p Full HD real-time video through a 2 mega pixel CMOS image sensor.

There is one camera in front of eye in the device. This camera records pupil reactions to light stimulus.

Specifications:

- Supports 1080p Full HD video at 30fps
- USB 2.0 port offers plug and- play setup,
- no software download/installation needed
- Compatible with all major third-party platforms, apps and softphones

- Adjustable video settings include brightness, resolution, saturation, contrast, low-light and more

Fig- 4.3 USB Web camera

4.1.2.2 Arduino UNO

Arduino is a software company, project and user community that designs and manufactures computer open source software and open source hardware and microcontroller based kits for building digital devices and interactive objects that can sense and control physics devices. Arduino provides an open source prototyping platform based on easy to use hardware and software. With the use of Arduino programming language (based on wiring, an open source programming framework which helps microcontroller boards to control devices attached to it) and Arduino software, we can give instructions to microcontroller board. With the help of these instructions we can tell an Arduino board what to do. Arduino boards are able to read those inputs (E.g.: Light on a sensor, a finger on a button or a twitter message) and turn it into an output (E.g.: Activating a motor, turning on an LED, publishing something online.

Arduino Nano present in the pupillometer device helps in programming the
LED's by (Telling, when each LED should be on, for how long they should be on, how many times they should be on and at what intensity should the brightness be) with the help of software, present in any computer or laptop to which this Arduino board is connected by a USB port. The instructions are given to this board about how the LED's should function.

Specifications:

- Operating Voltage (logic level): 5V.
- Microcontroller: Atmel AT mega 168 or AT mega 328.
- Input Voltage (recommended): 7 – 12 V.
- Input Voltage (limits): 6 – 20 V.
- Digital I/O Pins: 14 (out of which 6 provide PWM output).
- Analog Input Pins: 8.
- DC Current per I/O Pin: 40 Ma.
- Flash Memory: 16 KB (AT mega 168) or 32 KB (AT mega 328).
- Of which 2 KB is used by the Boot loader.
- SRAM: 1 KB (AT mega 168) or 2 KB (AT mega 328).
- EEPROM: 512 bytes (AT mega 168) or 1 KB (AT mega
- 328).
- Clock Speed: 16 MHz
- Dimensions: 0.73” x 1.70”.
- Length: 45mm.
- Width: 18mm.
- Weight: 5 gm.

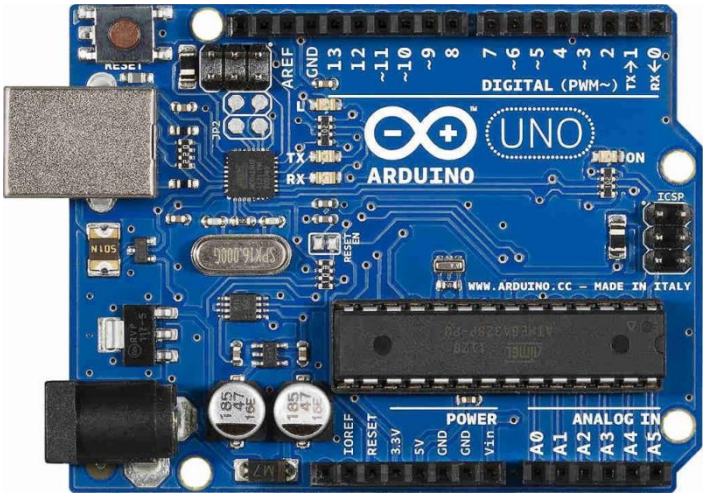

Figure 4.4 Arduino UNO

4.1.2.3 White LED's (Warm)

There are eight, white or visible LED's present in the device, four in front of each eye. They emit monochromatic light, occurring at a single wavelength.

Specifications:

• Shape: Round
• Emitting Colour: Warm white, Cool white
• Temp Colour: Warm white2800-3500k, Cool white 5000k-8000k
• Lens Colour: Water clear
• Life Span: 60,000 hours with RoHS & CE approved
•Luminous Brightness: White:2000mcd/6-7lm
• Beam Angle: 120 degrees
• Forward Voltage: 3.0-3.6V
• Forward Current: 20mA.
• LED radius: 5.0mm.

Figure: 4.5 White led's

4.1.2.4 Power Bank:

Ambrane Portable Charger P-1000(10400mAh) is Portable USB Power Bank with Dual USB ports. This is used to provide power supply to the Arduino UNO Board in the device.

Specifications:

• Connectors: Micro USB
• Brand: Ambrane
• Power Supply: 5V/1A
• Model Number: P-1000 Star
• Battery Capacity: 10400 mAh
• Model Name: Power Bank
• Output Power: 5V/1A, 5V/2.1A
• Power Source: Battery

Figure 4.6 Power bank

• Battery Type: Lithium-ion

• Output Current: 1A, 2.1A

4.1.2.5 Iris scanner

The iris is the coloured part of the eye that surrounds the pupil and contains intricate patterns of lines, dots, and other features that are unique to each individual.

Iris scanners typically use a camera or sensor to capture an image of the iris and then use specialized software to analyze the patterns and compare them to a stored database of iris images to verify the person's identity. This technology is widely used in security and access control systems, such as airports, government buildings, and high-security facilities.

Iris scanning is considered one of the most accurate forms of biometric identification because the patterns in the iris are stable throughout a person's life and are not affected by external factors such as aging, disease, or injury. Additionally, the iris has a very low false positive rate, meaning that it is highly unlikely for two individuals to have the same iris pattern.

Iris scanner proprietary distance sensing and focus analysis technology gives fast auto capture capabilities. Supports Windows, Linux and Android Operating Systems.

IRIS Scanner can be utilized widely for identity applications like Aadhaar Authentication, Banking Applications and Access Control Applications.

The major applications of biometric iris recognition technology involve restricting unauthorized access in the facilities, immigration at the airports, hospitals and clinics, border control system, to unlock various devices and smart phones, aviation security, various government schemes, and many more.

Figure 4.7 Single Iris scanner

4.1.3 software description

The different software tools used in the development of the custom designed software for the device are as described below.

4.1.3.1 Google colab

Google Colab is a cloud-based platform that can be used for building and training classifiers. A classifier is a machine learning model that learns to classify data into different categories or classes based on input features.

Using Google Colab, you can write and execute Python code to create and train classifiers. The platform provides access to powerful hardware resources, including GPUs and TPUs, which can significantly speed up the training process, especially for complex models and large datasets.

Colab supports popular machine learning libraries such as TensorFlow and PyTorch, allowing you to leverage their capabilities for building and training classifiers. These libraries provide various algorithms and techniques, such as deep learning neural networks, decision trees, support vector machines, and more, that can be used to develop effective classifiers.

In addition to the training process, Colab also provides tools for data preprocessing, visualization, and evaluation of classifiers. You can import datasets, perform data cleaning and feature engineering, visualize data distributions and relationships, and evaluate the performance of your classifiers using metrics such as accuracy, precision, recall, and F1 score.

With its collaborative and interactive nature, Google Colab allows you to share your classifier code and notebooks with others, making it a useful tool for collaborative machine learning projects and research.

4.1.3.2 Arduino UNO

The open-source Arduino Software (IDE) makes it easy to write code and upload it to the board. It runs on Windows, Mac OS X and Linux. The Arduino project provides the Arduino integrated development environment (IDE), which is a cross platform application written in the programming language Java. It originated from the IDE for the languages Processing and Wiring. It is designed to introduce programming to artists and other newcomers unfamiliar with software development. It includes a code editor with features

such as syntax highlighting, brace matching, and automatic indentation, and provides simple one-click mechanism to compile and load programs to an Arduino board. A program written with the IDE for Arduino is called a "sketch".

The Arduino IDE supports the languages C and C++ using special rules to organize code. The Arduino IDE supplies a software library called Wiring from the Wiring project, which provides many common input and output procedures. A typical Arduino C/C++ sketch consist of two functions that are compiled and linked with a program stub main () into an executable cyclic executive program:

· setup (): a function that runs once at the start of a program and that can initialize settings.

· loop (): a function called repeatedly until the board powers off.

After compiling and linking with the GNU toolchain, also included with the IDE distribution, the Arduino IDE employs the program avrdude to convert the executable 1005-14-740117 33 code into a text file in hexadecimal coding that is loaded into the Arduino board by a loader program in the board's firmware. Arduino programs may be written in any programming language with a compiler that produces binary machine code. Atmel provides a development environment for their microcontrollers, AVR Studio and the newer Atmel Studio, which can be used for programming Arduino. Arduino can be controlled using C/C++ interpreter Ch without the binary code.

4.1.3.3 Deep learning classifiers

Deep learning classifiers are machine learning models that use artificial neural networks with multiple layers to analyze and classify data. They have gained significant popularity due to their ability to automatically learn hierarchical representations from raw data, allowing them to capture complex patterns and make accurate predictions.

Here's a brief overview of common deep learning classifiers:

- Convolutional Neural Networks (CNNs): CNNs are commonly used for image classification tasks. They employ convolutional layers to extract local features from images and pooling layers to down sample the feature maps. Fully connected layers at the end of the network combine the extracted features to make predictions.
- Recurrent Neural Networks (RNNs): RNNs are suitable for sequential data analysis, such as natural language processing and time series prediction. They have recurrent connections that allow information to persist over time, enabling the network to capture temporal dependencies in the data.

- Long Short-Term Memory (LSTM) Networks: LSTMs are a type of RNN that address the vanishing gradient problem and can better capture long-term dependencies. They have a memory cell and three main gates (input, output, and forget) that control the flow of information within the network.
- Gated Recurrent Unit (GRU) Networks: GRUs are another variant of RNNs that simplify the LSTM architecture by combining the input and forget gates. They have a more streamlined structure and are computationally more efficient.
- Transformer Networks: Transformers have revolutionized natural language processing tasks. They use self-attention mechanisms to capture relationships between different words in a sentence without sequential processing. Transformers have shown excellent performance in tasks like machine translation and text classification.

4.2 Data Collection

The data collection process for measuring the pupil using a pupillometer for relative afferent pupillary defect (RAPD) typically involves the following steps:

1. Subject Preparation: Prepare the subject for the examination by ensuring they are in a comfortable position and their eyes are relaxed. Inform the subject about the procedure and obtain their consent.
2. Lighting Conditions: Ensure consistent lighting conditions in the examination area. Avoid bright or dim lighting that could affect the pupil size.
3. Baseline Measurement: Obtain a baseline measurement of the subject's pupils to establish the normal size and reactivity. This is usually done by directing the pupillometer towards the subject's eyes and capturing the initial pupil size.
4. Stimulus Presentation: Introduce the light stimulus to each eye separately to assess the relative afferent pupillary response. This can be done by using a flashing light, swinging flashlight, or other appropriate stimuli. Present the stimulus to one eye while observing the response of both pupils
5. Pupil Measurement: Use the pupillometer to measure the size and reactivity of the pupil during the stimulus presentation. The device will capture data such as the initial pupil size, constriction velocity, latency, and dilation velocity. Repeat the measurement for each eye separately.

6. Recording and Documentation: Record the measurements obtained from the pupillometer for each eye. Include relevant information such as the subject's identification, date, time, presence of defects such as cataract, blurry vision or otherwise normal vision.

Fig:4.8 Collecting data at Kantivelugu programme

The below shown images are captured using iris scanner at Kantivelugu programme which are being used for further analysis.

Figure 4.9 Subject 1 LE_WS

Figure 4.10 Subject 1 RE_WS

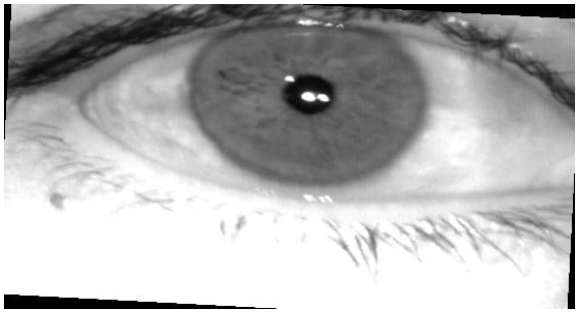

Figure 4.11 Subject-1 LE_S

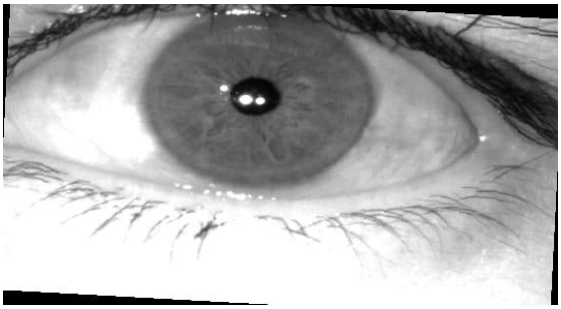

Figure 4.12 Subject-1 RE_S

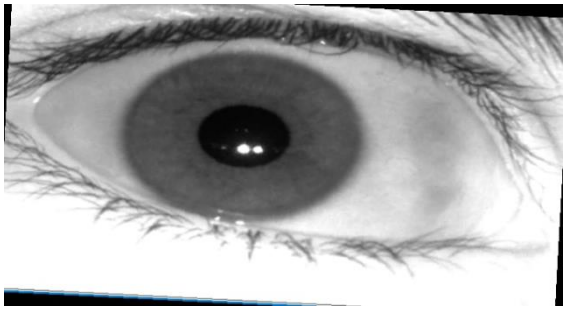

Figure 4.13 Subject-2 LE_WS

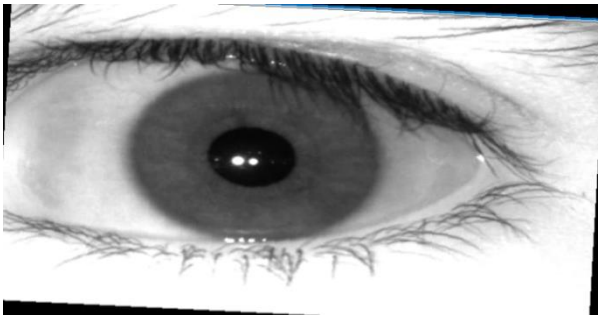

Figure 4.14 Subject-2 RE_WS

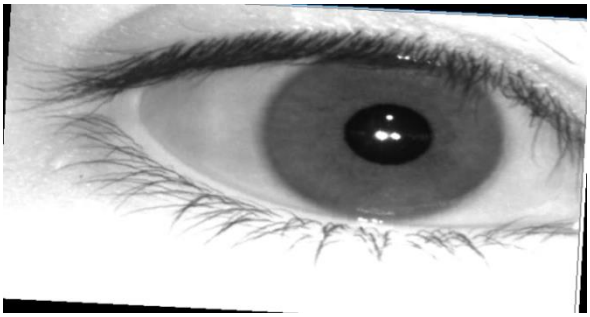

Figure 4.15 Subject-2 LE_S

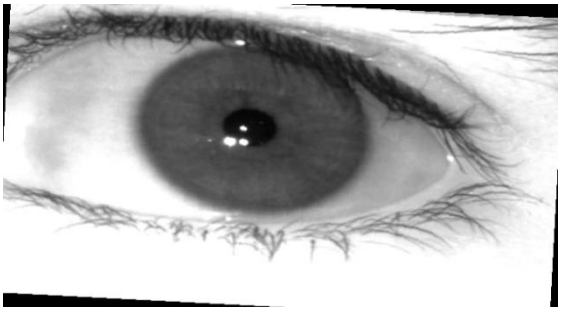

Figure 4.16 Subject-2 RE_S

While taking the images of pupil from subjects the basic information like name age is recorded in excel sheet as shown below

S.NO	NAME	AGE	G	EXISTING DISEASES IF ANY			RAPD	
				B.P	DIABETES	CATARACT	DARK VISION	LIGHT VISION
1	B.Balamani	53	F	YES	YES	NO	CLEAR	CLEAR
2	S.Vijay kumarN	45	M	NO	NO	NO	CLEAR	CLEAR
3	K.Shankar	52	M	NO	NO	YES	BLURRY VISION	BLURRY VISION
4	Wjida Begum	30	F	NO	NO	NO	CLEAR	CLEAR
5	A.Venkataiah	38	M	NO	NO	NO	CLEAR	CLEAR
6	A.Indu	23	F	NO	NO	NO	CLEAR	CLEAR
7	P.Prasanna	45	F	NO	NO	YES	CLEAR	CLEAR
8	B.Devadanam	50	M	NO	NO	YES	BLURRY VISION	BLURRY VISION
9	MD.Ayub	44	M	NO	NO	NO	CLEAR	CLEAR
10	K.Sagar	50	M	NO	NO	NO	CLEAR	CLEAR
11	C.Praveen Kumar	34	M	YES	NO	NO	CLEAR (HEAD ACHE)	CLEAR (HEAD ACHE)
12	K.Rukmaiah	71	M	N0	YES	YES	CLEAR	CLEAR
13	B.Ramulamma	56	F	NO	NO	YES	CLEAR	CLEAR
14	A.Indira Devi	69	F	YES	YES	YES	CLEAR	CLEAR
15	Mohammed Anwar Khan	53	M	NO	NO	YES	CLEAR	CLEAR
16	J.Meghana	18	F	NO	NO	NO	CLEAR	CLEAR
17	CH.Uday Kumar	17	M	NO	NO	NO	CLEAR	CLEAR
18	R.Navaneetha	40	F	NO	NO	NO	BLURRY VISION	BLURRY VISION
19	Sahera Begum	62	F	NO	NO	YES	CLEAR	CLEAR
20	Sulthana Begum	40	F	NO	NO	NO	CLEAR	CLEAR
21	V.Lalitha	57	F	NO	NO	YES	CLEAR	CLEAR
22	MD. Mahmood	75	M	NO	YES	YES	CLEAR	CLEAR
23	MD.Naseer	56	M	NO	NO	YES	CLEAR	CLEAR
24	B.JAYA	55	F	YES	YES	NO	CLEAR	CLEAR
25	B.Jagadish	65	M	NO	YES	YES	CLEAR	CLEAR
26	CH.Surya Kumari	40	F	NO	NO	YES	CLEAR	CLEAR
27	E.S.N. Teja Swaroop	12	M	NO	NO	NO	CLEAR	CLEAR
28	E.S. NARENDER SWAROOP	52	M	NO	YES	NO	CLEAR	CLEAR
29	M.Sai Kumar	42	M	NO	NO	NO	CLEAR	CLEAR
30	B.Amba Das	48	M	YES	NO	NO	BLURRY VISION	BLURRY VISION
31	Syed Akbar	70	M	YES	YES	YES	BLURRY VISION	BLURRY VISION

32	Asadhullah Khan	46	M	YES	NO	YES	CLEAR	CLEAR
33	Humera Begum	40	F	NO	NO	NO	CLEAR	CLEAR
34	MOHAMAD UMAR	61	M	YES	YES	YES	RIGHT EYE DEFECT	RIGHT EYE DEFECT
35	D.Krishna	43	M	NO	NO	YES	CLEAR	CLEAR
36	T.Bala Chander Rao	43	M	NO	NO	NO	CLEAR	CLEAR
37	E.Laxmi	39	F	NO	NO	YES	CLEAR	CLEAR
38	G.Rani	42	F	NO	NO	YES	CLEAR	CLEAR
39	K.Archana	31	F	NO	YES	NO	CLEAR	CLEAR
40	N.Kundan bai	74	F	YES	NO	YES	WATERY EYE	WATERY EYE
41	K.Bala krishna	40	M	NO	YES	NO	UNCLEAR DURING BIKE RIDE	CLEAR
42	G.Mounika	27	F	NO	NO	NO	CLEAR	CLEAR
43	N.Mamatha	30	F	NO	NO	NO	CLEAR	CLEAR
44	E.Yashodha	48	F	NO	NO	NO	CLEAR	CLEAR
45	K.Kanakatara	69	F	YES	NO	YES	BLURRY VISION	CLEAR
46	G.Dhanu sri	15	F	NO	NO	NO	LEFT EYE DEFECT	CLEAR
47	B.BALAMANI	64	F	YES	YES	YES	CLEAR	CLEAR
48	G.PAVAN	45	M	YES	NO	NO	CLEAR	CLEAR
49	D.PRAMILA	58	F	NO	NO	YES	CLEAR	CLEAR
50	V.SAROJA	50	F	NO	NO	YES	CLEAR	CLEAR
51	E.YELLAIAH	58	M	NO	NO	NO	CLEAR	CLEAR
52	P.JAMUNA	42	F	NO	NO	NO	DEFFECT	DEFECT
53	V.SATHYANA RAYANA	65	M	NO	NO	YES	DEFECT	CLEAR
54	ZAHEEDA BEGUM	52	F	YES	YES	YES	DEFECT	DEFECT
55	ASMA BEGUM	22	F	NO	NO	NO	CLEAR	CLEAR
56	S.PREMA LATHA	50	F	YES	NO	YES	CLEAR	DEFECT
57	T.ANJANA DEVI	72	F	NO	NO	YES	CLEAR	CLEAR
58	N.KASAIAH	52	M	NO	NO	YES	CLEAR	CLEAR
59	G.BHAVANA	35	F	NO	NO	NO	CLEAR	CLEAR
60	K.SANTOSHAMMA	46	F	NO	NO	NO	BLURRY VISION	CLEAR
61	G.BLESSY	11	F	NO	NO	NO	CLEAR	CLEAR
62	K.SANGEETHA	23	F	NO	NO	NO	CLEAR	DEFECT
63	G.VANITHA	42	F	NO	NO	YES	CLEAR	CLEAR
64	NAZEEMA	40	F	NO	NO	NO	CLEAR	CLEAR
65	D.NARAHARI	48	M	NO	YES	YES	DEFECT	BLURRY VISION

66	K.REEMA SREE	16	F	NO	NO	NO	DEFECT	BLURRY VISION
67	K.JYOTHI	40	F	YES	NO	NO	CLEAR	CLEAR
68	A.RATHNAM ALA	47	F	NO	NO	NO	CLEAR	CLEAR
69	D.HARI KRISHNA	63	M	NO	NO	NO	CLEAR	CLEAR
70	TAHASEEN SULTHAN	40	F	YES	NO	NO	CLEAR	DEFECT
71	P. MANEMMA	59	F	YES	NO	YES	CLEAR	CLEAR
72	CH.LAKSHMI	68	F	YES	NO	YES	CLEAR	CLEAR
73	K.YADAGIRI	53	M	YES	YES	YES	CLEAR	CLEAR
74	V.BHAGYA LAKSHMI	52	F	YES	YES	NO	CLEAR	CLEAR
75	FARANA SULTHANA	22	F	NO	NO	NO	CLEAR	CLEAR
76	P.NARASIMH A CHARY	73	F	YES	NO	NO	CLEAR	DEFECT
77	S.BALAMANI	45	F	NO	NO	NO	CLEAR	CLEAR
78	J.YADHAIAH	79	M	YES	NO	YES	CLEAR	CLEAR
79	T.SUGUNA	45	F	NO	YES	NO	CLEAR	CLEAR
80	D,POCHAIAH	52	M	NO	YES	YES	CLEAR	CLEAR
81	J.BHAGYA LAKSHMI	43	F	NO	NO	NO	CLEAR	CLEAR
82	ARCHIT REDDY	12	M	NO	NO	NO	CLEAR	CLEAR
83	T.SRINIVAS	48	M	YES	YES	YES	BLURRY VISION	BLURRY VISION
84	NAJMA UNNISA	41	F	NO	NO	YES	BLURRY VISION	CLEAR
85	MD KHALIS	37	M	YES	NO	NO	CLEAR	DEFECT
86	S.CHENNAM MA	55	F	NO	NO	YES	BLURRY VISION	BLURRY VISION
87	K.MANIKYA REDDY	56	M	NO	NO	NO	CLEAR	CLEAR
88	M.ANWAR HUSSAIN	54	M	NO	NO	NO	CLEAR	CLEAR
89	N.SARITA	34	F	NO	NO	NO	CLEAR	CLEAR
90	K.VINOD KUMAR	43	M	YES	YES	NO	CLEAR	CLEAR
91	SONU RATHOD	36	F	NO	NO	NO	CLEAR	CLEAR
92	FATIMA FIRDOUS	38	F	YES	NO	NO	CLEAR	CLEAR
93	FAHMIDA BEGUM	43	F	NO	NO	NO	CLEAR	CLEAR
94	SHAMEEM BEGUM	45	F	NO	NO	NO	BLURRY VISION	CLEAR
95	R.MANJU	52	F	NO	NO	YES	NO	CLEAR
96	D.SHANTHA BAI	58	F	NO	NO	YES	CLEAR	CLEAR
97	SRI RAM YADAGIRI	51	M	NO	NO	YES	CLEAR	CLEAR

98	S. RAJA MANI	37	F	NO	NO	NO	DEFECT OF LEFT EYE DUE TO INJURY	DEFECT OF LEFT EYE DUE TO INJURY
99	MD BHASIR BHANU	35	F	NO	NO	NO	CLEAR	CLEAR
100	SAYED NAZEER	52	M	NO	NO	YES	CLEAR	CLEAR
101	B.MOHAN DAS	65	M	YES	YES	YES	CLEAR	CLEAR
102	G.NIRMALA	55	F	YES	YES	YES	CLEAR	CLEAR
103	M.LALITHA DURGA	30	F	NO	NO	NO	CLEAR	CLEAR
104	G.SWAPNA	37	F	NO	NO	NO	CLEAR	DEFECT
105	B.PUSHPA	60	F	YES	YES	NO	CLEAR	CLEAR
106	D.RAMESH	41	M	YES	YES	NO	CLEAR	CLEAR
107	L.SAI PRANAV	13	M	NO	NO	NO	CLEAR	CLEAR
108	L.LALITHA	56	F	NO	NO	YES	CLEAR	CLEAR
109	P.JAGADAMBA	45	F	NO	NO	NO	CLEAR	BLURRY VISION
110	MD IQBAL	51	M	NO	NO	NO	CLEAR	CLEAR
111	SHAHZADI BEGUM	77	F	YES	YES	YES	CLEAR	CLEAR
112	AZMATH BEGUM	42	F	YES	NO	NO	CLEAR	CLEAR
113	K.VINEETHA	36	M	NO	NO	NO	BLURRY VISION	DEFECT
114	SHAKUNTHALA	82	F	NO	NO	YES	BLURRY VISION	CLEAR
115	B.RAJ KUMAR	52	M	NO	NO	NO	CLEAR	CLEAR
116	B.NEERJA KUMARI	50	F	YES	NO	YES	CLEAR	CLEAR
117	G.PRAVEEN KUMAR	48	M	NO	NO	NO	CLEAR	CLEAR
118	D.GAYATHRI	13	F	NO	NO	NO	CLEAR	CLEAR
119	V.JAYA LAKSHMI	57	F	YES	NO	YES	DEFECT	DEFECT
120	NASREEN KHATHUM	37	F	NO	NO	NO	CLEAR	CLEAR
121	D.RADHIKA	31	F	NO	NO	NO	CLEAR	CLEAR
122	P.KRISHNA	50	M	NO	NO	NO	CLEAR	CLEAR
123	J,LAVANYA	46	F	NO	NO	NO	CLEAR	CLEAR
124	J.KEERTHI SAI	22	F	NO	NO	NO	CLEAR	CLEAR
125	BALAJI	34	M	NO	NO	NO	CLEAR	CLEAR
126	G.SRINIVAS	45	M	YES	NO	YES	CLEAR	CLEAR

4.2 Data Representation

4.2.1 Collected data

Total number of patients – 535

Gender	Number of Patients
Males	**298**
Females	**237**

Tabel 1 Gender reference classification of dataset

Age Range	Number of patients
10-19	**71**
20-29	**138**
30-39	**159**
40-49	**104**
50-80	**63**

Tabel 2 Age reference classification of dataset

Vision	Number of Patients
Catract	**86**
Normal	**278**
Blurred	**171**

Tabel 3 Vision defect reference classification of dataset

4.3 Feature Extraction

1. The image is captured using the device, the captured image will be in the form of PNG file.
2. Png file is converted into the JSON file, because in JSON file the structured data is converted into the human readable data, the JSON file also includes the file location, coordinates (longitudes & latitudes).
3. The points from the annotation file are obtained, the points which are obtained from the annotation file are used to define the feature with in the range of image, these obtained points are assigned to the variable x.
4. The variable x is provided as the input.
5. A variable is assigned as length of x, it is mainly used to resize and re-shaping of the image to meet the input requirements of the feature extraction model.
6. If the length of the mask is equal to 0 , that means no pupil is detected then it returns to 0.
7. If the length of the mask is greater than 0, then it means that the pupil is detected and it starts the procedure to draw the contours.
8. The mask array is multiplied with 255, this is done to convert the mask array into int unit8.
9. By converting the mask array to Int unit 8, we can obtain the memory efficiency and converting it into 8 bit binary image.
10. The contours are drawn on the masked image by using the 2 methods that include:
    Contour approximation method: Contour approximation is a technique used to simplify the representation of a contour by reducing the number of points required to define it. It helps in reducing computational complexity and can be useful for tasks like object recognition or shape analysis. One common algorithm used for contour approximation is the Douglas-Peucker algorithm. It recursively simplifies a contour by removing points that deviate minimally from the overall shape.
    Contour retrieval method: Contour retrieval involves grouping and organizing contours based on their hierarchical relationships. It is particularly useful when dealing with complex scenes or objects with nested structures. Contour retrieval methods typically operate on a contour hierarchy or tree-like structure.
11. These obtained contour points are stored in a variable.

12. The contours are drawn from the obtained points which are stored in a variable on the mask image array.
13. Finding the minimum enclosing circle and radius in feature extraction typically refers to a technique used to determine the smallest circle that can encompass a set of features or data points.
14. Returning the radius in feature extraction refers to providing the calculated radius value as a result of the feature extraction process.

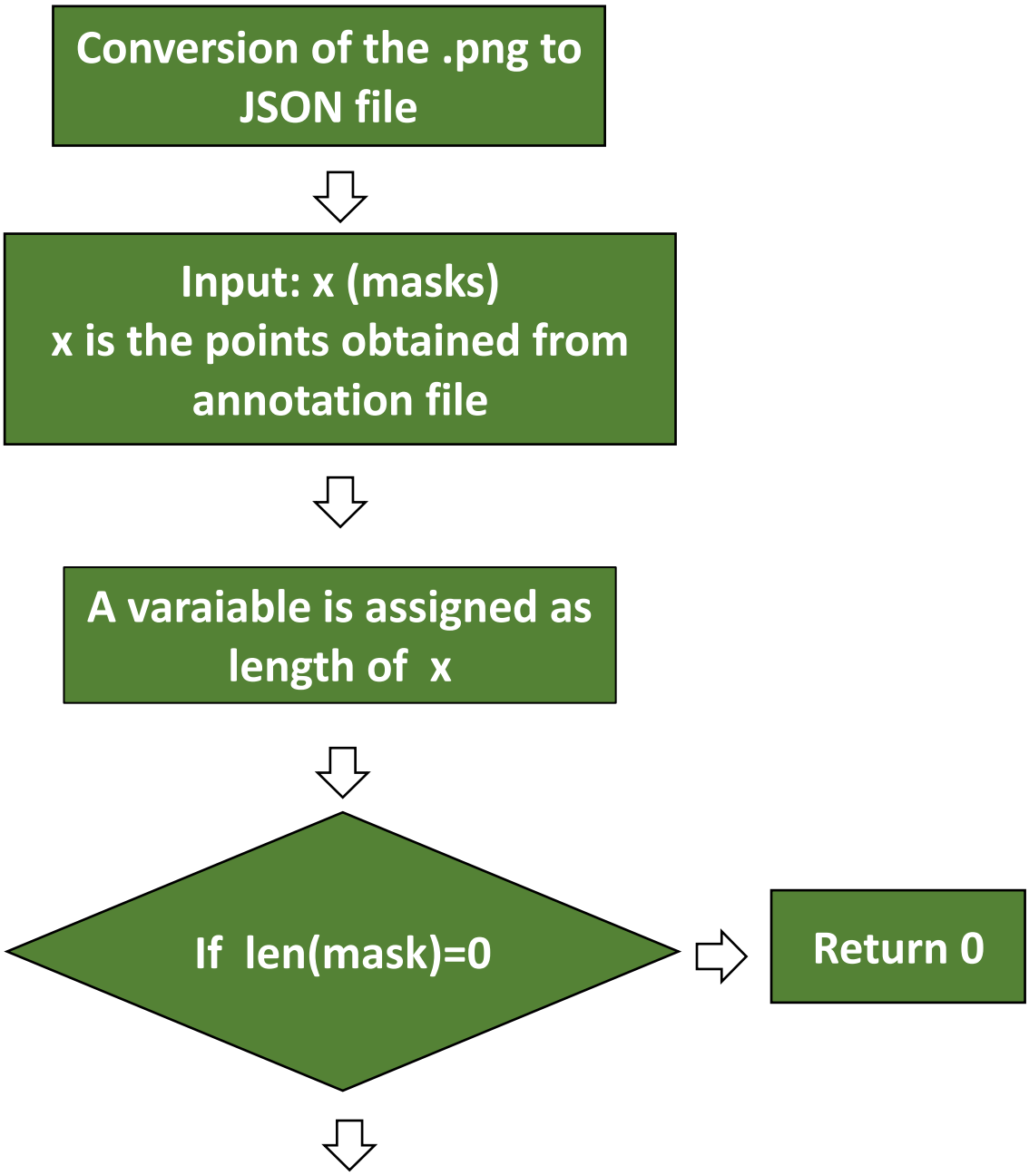

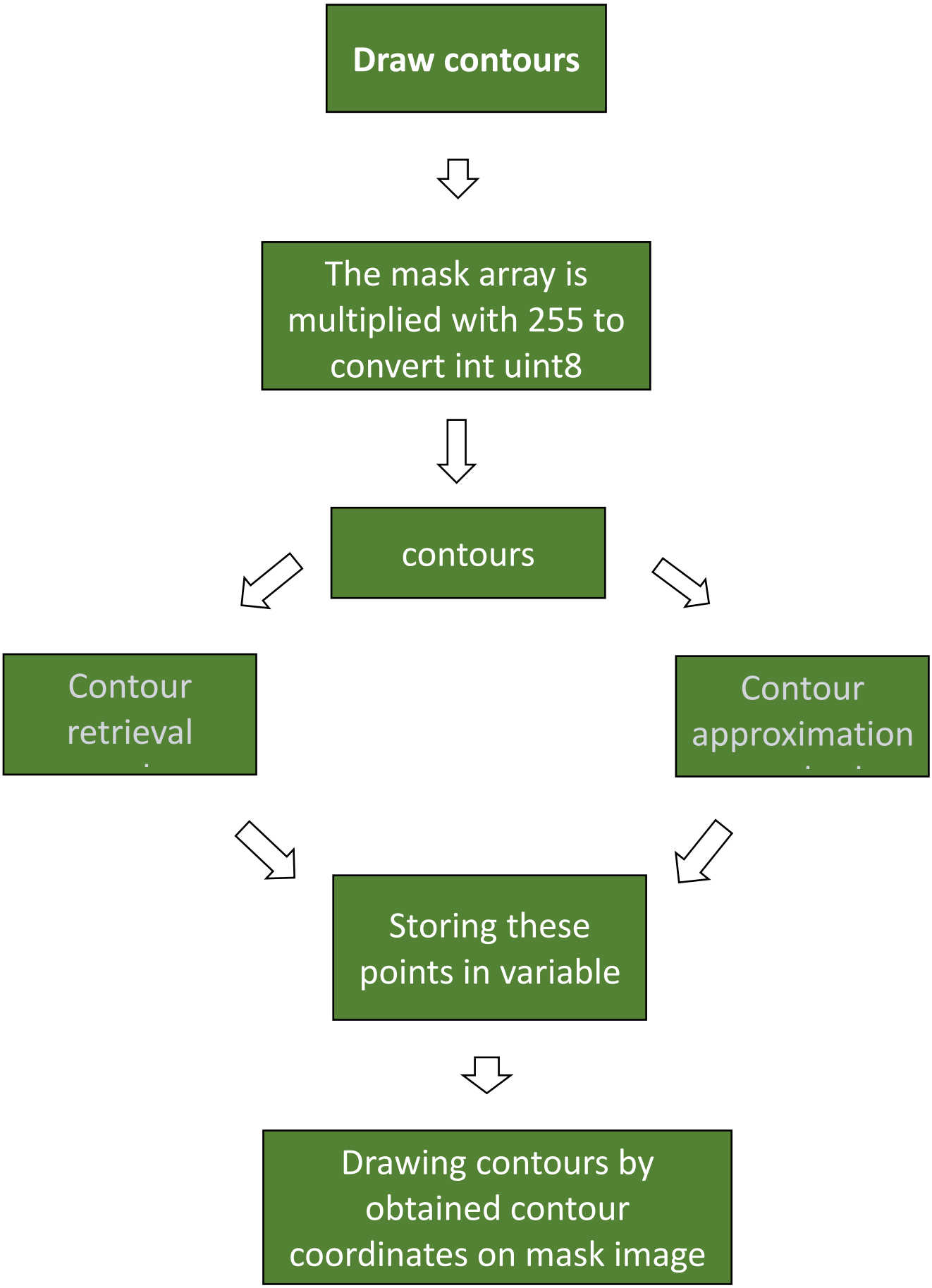
Draw contours
The mask array is multiplied with 255 to convert int uint8
contours
Contour retrieval
Contour approximation
Storing these points in variable
Drawing contours by obtained contour coordinates on mask image

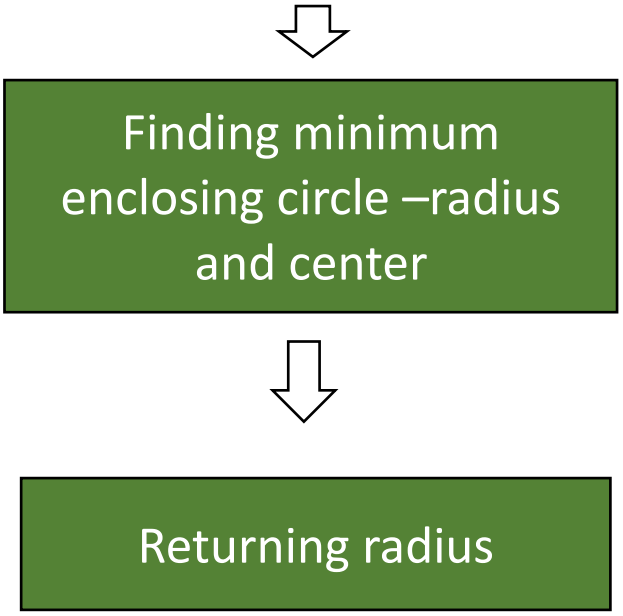

4.3.1 Libraries required for Feature Extraction

Pytorch

PyTorch is a popular deep learning framework that provides a flexible and efficient platform for building and training deep neural networks. It offers a wide range of features and functionalities that make it well-suited for deep learning tasks. Here are some key aspects of PyTorch in the context of deep learning:

Dynamic Computation Graph: PyTorch uses a dynamic computation graph, which allows for dynamic graph construction during runtime. This dynamic nature enables more flexibility in model design and facilitates techniques such as recurrent neural networks (RNNs) and attention mechanisms. It also simplifies debugging and model development.

Tensors and Automatic Differentiation: PyTorch is built around tensors, which are multi-dimensional arrays that can represent numerical data. Tensors in PyTorch are similar to NumPy arrays but have additional capabilities such as automatic differentiation. Automatic differentiation enables the calculation of gradients automatically, which is crucial for training deep learning models through backpropagation.

Model Building and Training: PyTorch provides a high-level API for defining and training deep learning models. The torch.nn module offers a wide range of pre-defined layers (e.g., convolutional layers, fully connected layers, recurrent layers) that can be easily composed to build complex architectures. PyTorch also provides tools for managing training loops,

calculating loss functions, and optimizing models using various optimization algorithms (e.g., SGD, Adam).

GPU Acceleration: PyTorch seamlessly integrates with GPUs, allowing for accelerated training and inference on GPU devices. It provides a simple interface for moving data and models to GPUs, enabling efficient computation on large-scale datasets and complex models.

Model Deployment: PyTorch provides tools and utilities for model deployment, including model serialization and loading, model quantization for deployment on resource-constrained devices, and integration with other deployment frameworks such as ONNX and TensorFlow.

Extensive Community and Ecosystem: PyTorch has a large and active community of researchers and developers, resulting in a rich ecosystem of libraries, pre-trained models, and resources. This ecosystem includes libraries like torchvision for computer vision tasks, torchtext for natural language processing, and various domain-specific libraries for specific applications.

OpenCV (Open Source Computer Vision Library)

OpenCV can play a significant role in feature extraction in computer vision tasks, including those related to deep learning. Here are some ways OpenCV can contribute to feature extraction:

1. Preprocessing and Image Enhancement: OpenCV provides a wide range of image processing functions that can be used for preprocessing and enhancing images before feature extraction. This includes operations such as resizing, cropping, smoothing, sharpening, histogram equalization, and noise removal. These preprocessing steps can help improve the quality and clarity of images, which in turn can enhance the accuracy of feature extraction algorithms.
2. Feature Detection and Extraction Algorithms: OpenCV includes various feature detection and extraction algorithms that can be used to identify and extract key features from images. For example, OpenCV provides functions for detecting corners using the Harris corner detector or the Shi-Tomasi corner detector. It also offers algorithms for extracting local features using methods like SIFT (Scale-Invariant Feature Transform), SURF (Speeded-Up Robust Features), or ORB

(Oriented FAST and Rotated BRIEF). These features can serve as valuable input for subsequent analysis or machine learning algorithms.

3. Object Detection and Tracking: OpenCV offers object detection and tracking algorithms that can assist in extracting features related to specific objects or regions of interest. Techniques like Haar cascades, HOG (Histogram of Oriented Gradients), and template matching can be used to identify and track objects in images or video streams. These algorithms can be valuable for tasks such as facial recognition, object tracking, or gesture recognition.
4. Image Segmentation: OpenCV provides segmentation algorithms that can separate an image into different regions based on common visual characteristics. Segmentation can help in extracting meaningful features by isolating objects or regions of interest. OpenCV offers methods like GrabCut, Watershed, or contour-based segmentation for this purpose.
5. Feature Visualization: OpenCV facilitates the visualization of extracted features by providing functions for drawing overlays, bounding boxes, or contours on images. This allows for a visual representation of the extracted features and their spatial distribution within an image.
6. Integration with Deep Learning: OpenCV can be integrated with deep learning frameworks like PyTorch or TensorFlow to leverage its feature extraction capabilities alongside deep neural networks. OpenCV can preprocess images, extract features, and provide inputs to deep learning models for further analysis or classification.

NumPy (Numerical Python)

NumPy plays a crucial role in feature extraction using deep learning by providing essential functionalities for data manipulation, numerical computations, and linear algebra operations. Here's how NumPy contributes to feature extraction in deep learning:

1. Data Representation: NumPy arrays serve as the fundamental data structure for representing and manipulating data in deep learning. Deep learning models often operate on multi-dimensional arrays (tensors) as input data. NumPy allows for efficient creation, manipulation, and slicing of arrays, making it easier to handle and preprocess the input data for feature extraction.
2. Data Preprocessing: Feature extraction typically involves preprocessing the input data to enhance its quality or normalize it. NumPy provides various functions for

data preprocessing tasks, such as scaling, normalization, and standardization. These functions allow for efficient and vectorized computations on large datasets, preparing the data for feature extraction algorithms.

3. Array Operations: NumPy provides a rich set of mathematical and array operations that are essential for feature extraction. These operations include element-wise operations (e.g., addition, subtraction, multiplication), broadcasting, slicing, and indexing. These operations enable efficient manipulation and processing of the input data, extracting relevant features for further analysis.
4. Numerical Computations: NumPy offers a wide range of mathematical functions that are useful in feature extraction. These functions include statistical operations, trigonometric functions, exponential functions, logarithmic functions, and more. These numerical computations can be applied to the input data to extract meaningful features or perform transformations that enhance the discriminative power of the features.
5. Linear Algebra Operations: Many feature extraction techniques in deep learning rely on linear algebra operations, such as matrix multiplications, matrix factorizations, and eigenvalue computations. NumPy provides efficient implementations of these operations, enabling the extraction of features using linear algebra-based algorithms like PCA (Principal Component Analysis), SVD (Singular Value Decomposition), or LDA (Linear Discriminant Analysis).
6. Integration with Deep Learning Frameworks: NumPy seamlessly integrates with popular deep learning frameworks such as PyTorch and TensorFlow. Deep learning frameworks often use NumPy arrays as the standard data format for input and output data. NumPy's compatibility with these frameworks allows for easy integration of feature extraction algorithms into the deep learning pipeline.

Detectron2

Detectron2, as a flexible and modular computer vision library built on top of PyTorch, can be leveraged for pupil detection using deep learning. While Detectron2 is primarily designed for object detection and instance segmentation tasks, it can be adapted and utilized for pupil detection with some modifications and considerations. Here are the key roles of Detectron2 in pupil detection using deep learning:

1. Model Architecture: Detectron2 provides a wide range of pre-defined model architectures for object detection and instance segmentation. These architectures,

such as Faster R-CNN and Mask R-CNN, can serve as a starting point for building a pupil detection model. By adapting the network architecture and modifying the output layers, the model can be trained to detect and localize the pupil in eye images.

2. Data Loading and Pre-processing: Detectron2 offers efficient data loading and pre-processing functionalities. It supports common image formats and provides tools for data augmentation, resizing, and normalization. These capabilities are crucial for preparing the training and testing datasets for pupil detection tasks, ensuring that the input images are properly processed before feeding them into the deep learning model.
3. Training and Fine-tuning: Detectron2 provides training capabilities for deep learning models. It supports both single-GPU and multi-GPU training, allowing for efficient utilization of computational resources. With Detectron2, you can define the training configurations, including the learning rate, optimizer, and number of training iterations. Fine-tuning pre-trained models from the Detectron2 Model Zoo or training models from scratch on pupil detection datasets can be performed using the provided training framework.
4. Evaluation and Metrics: Detectron2 includes evaluation tools and metrics for assessing the performance of the pupil detection model. It provides evaluation metrics such as mean Average Precision (mAP), which measures the accuracy of object detection, and Average Recall (AR), which evaluates the model's ability to detect the pupil across different scales and orientations. These metrics help in quantifying the performance of the pupil detection model and comparing different model variants or training configurations.
5. Visualization and Analysis: Detectron2 offers visualization tools to inspect and analyze the results of pupil detection. You can visualize the predicted bounding boxes or keypoints of the detected pupils overlaid on the input images. This allows for visual verification and interpretation of the model's performance. Additionally, you can analyze the model's output confidence scores and refine the detection threshold based on the desired trade-off between precision and recall.

4.4 Classification

4.4.1 Classifiers used for classifying the data:

Scikit-learn (also known as sklearn) is a popular machine learning library in Python that provides a wide range of tools and algorithms for various machine learning tasks, including deep learning. While scikit-learn is primarily focused on traditional machine learning algorithms, it can still be useful in the context of deep learning in several ways:

1. Data Preprocessing: Scikit-learn offers a comprehensive set of functions and classes for data preprocessing tasks, such as feature scaling, dimensionality reduction, handling missing values, and encoding categorical variables. These preprocessing techniques are often applied before feeding the data into deep learning models to improve their performance and convergence.
2. Pipeline Construction: Scikit-learn provides a convenient Pipeline class that allows you to assemble multiple preprocessing steps and a machine learning model into a single object. This can be useful when combining traditional feature extraction techniques with deep learning models. For example, you can use scikit-learn to preprocess image data or extract features and then pass the transformed data to a deep learning model.
3. Model Evaluation and Selection: Scikit-learn offers a variety of evaluation metrics and techniques for assessing the performance of machine learning models. These metrics, such as accuracy, precision, recall, and F1-score, can be used to evaluate the performance of deep learning models as well. Scikit-learn also provides functions for cross-validation, hyperparameter tuning, and model selection, which can be valuable in the iterative process of training and optimizing deep learning models.
4. Ensemble Methods: Scikit-learn includes ensemble learning methods, such as random forests, gradient boosting, and AdaBoost, which can be combined with deep learning models to improve their predictive accuracy or handle complex tasks. Ensemble methods can be used in conjunction with deep learning models to combine their predictions and leverage their respective strengths.
5. Transfer Learning: Although scikit-learn is not specifically designed for deep learning, you can still benefit from transfer learning using pre-trained models. By integrating scikit-learn with deep learning frameworks like TensorFlow or PyTorch,

you can leverage pre-trained deep learning models, such as those trained on ImageNet, for feature extraction or transfer learning tasks. Scikit-learn provides an interface to incorporate deep learning models into its pipeline, allowing for seamless integration.

While scikit-learn is not primarily focused on deep learning algorithms, it complements deep learning frameworks by providing a wide range of tools and techniques for data preprocessing, model evaluation, and ensemble methods. It can be used alongside deep learning libraries to enhance the overall machine learning workflow, including data preparation, model selection, and evaluation.

4.4.2 Steps under classification

1. The dataset obtained is converted into test data and train data.
2. The test data and train data are further divided into test_x, test_y and train_x, train_y.
3. The x contains the radius of right and left under stimulus and no stimulus conditions.
4. The y contains the classes of differentiation- normal, cataract and blurred.
5. label encoding of y values.
6. Define the file path to save the model.
7. After creating the Random Forest Classifier object, you can fit the classifier to your training data using the fit method. This step trains the model on the provided data, allowing it to learn patterns and make predictions. Once the model is trained, you can use the prediction method to make predictions on new, unseen data (Xtest in this example).
8. The corresponding accuracy, precision, recall scores are obtained.

The below is a test_x data which consists of about 406 subjects

S No	Patient	WS_LE_radius	S_LE_radius	WS_RE_radius	S_RE_radius
1	A.RAJASHEKAR	51.83199692	42.4374504	42.66751862	43.416687
2	S.VIJAY KUMAR	21.50375175	30.7612763	33.14728928	28.4430237
3	C.SHARANYA	53.03551102	74.7848129	76.8477478	55.4034538
4	D.ASHWINI	67.64892578	43.2816505	56.48461151	48.6622009
5	K.SHAMALA	54.74039459	42.3118744	58.03182602	46.9313126
6	H.RAMACHANDER	53.76776886	38.4708672	52.28059387	45.6208191

7	G.PRAVEEN KUMAR	54.39921188	31.9766522	46.0604248	32.2685051
8	J.M. MALLESWARI	30.11208916	27.2856274	30.51704025	26.8242111
9	K.ARCHANA	54.28973007	36.3456612	56.14277267	35.8538437
10	C.JAYASREE	73.54730988	44.4448471	71.39234161	46.9533005
11	V.BHAGYA LAKSHMI	42.7376709	34.6158485	44.22961426	35.0928421
12	FATIMA FIRDOUS	38.9040947	35.9271812	40.19960022	33.8009872
13	MD.SAMERUDDIN	42.57356644	36.7737045	41.25857925	36.7186241
14	N.RITESH RAJ	56.00683594	48.7044334	72.06430817	50.2245941
15	B.SHAILAJA	71.40274811	45.2355957	65.11537933	47.5996971
16	FARHEEN BEGUM	58.76639175	46.0978203	56.47612	49.2393112
17	M.SAVITHA	55.57887268	40.8843079	49.56195831	43.9119415
18	MAIMUNNNISSA BEGUM	49.17898178	39.2725105	46.63237762	39.1831627
19	K.PADMA	46.74162292	43.8361206	51.90867233	39.2588577
20	N.MANOGNA	64.51587677	47.7550659	61.66875458	52.407196
21	K.BHAGYAVATHI	47.73656464	37.2626801	43.59710693	37.2989922
22	C.PEEYUSHA	63.78293228	40.3397217	72.26696777	49.9250412
23	T.SUGUNA	39.13459015	36.0902634	33.39206314	34.4420776
24	M.ANWAR HUSSAIN	42.05481339	33.2024345	40.52478409	34.6195831
25	MD.AYUB	24.23406601	28.4838047	44.10225296	30.5000992
26	V.JAYA	34.34872818	26.2135754	30.70949745	22.9455185
27	A.SURENDER	38.20952988	34.9357529	40.20904541	30.0094204
28	MAHEEN	51.3352356	40.3764534	69.79444122	36.4966736
29	K.JYOTHI	36.89625168	28.7142067	47.22687531	37.9854202
30	BAHADOOR HANDER SINGH	38.83307648	32.8863449	34.70928955	34.9226685
31	SY.MD.DILAWAR KHAN	46.61026001	40.2027435	39.65485764	41.0200501
32	MD.FARIDUDDIN	35.72473907	33.1437264	34.36014175	27.0648365
33	S.BALAMANI	44.902771	38.3960609	45.30218124	36.4318543
34	B.BHAVANI	48.50384521	42.3586884	64.99433136	58.1765633
35	FARANA SULTHANA	75.40732574	44.7048836	74.9790802	48.9363327
36	E.YELLAIAH	54.34160995	36.8409729	52.31724548	40.9452438
37	T.ALIVELU	53.32263947	44.4187622	56.24562073	42.5794373
38	E.S.NARENDER SWAROOP	36.51074219	30.0542564	37.65987396	26.8765049
39	B.RAJ KUMAR	44.84149933	30.2320671	35.22792816	35.2279282
40	G.MANISHWAR	63.04201889	55.272583	76.69755554	52.153717
41	P.ANJAIAH	35.28820038	37.3364067	35.72473907	32.0704842

42	SHAIK SARABEE	63.57796478	49.3334312	69.35426331	52.9009514
43	D.GAYATHRI	41.93159103	34.3657799	60.42801285	48.5078316
44	MOUNIKA	62.3900032	43.6034241	58.27959824	33.3767395
45	NAYEEMA BEGUM	54.13920593	52.0284042	47.68689346	39.3224831
46	A.LAXMI NARASIMHA	53.35512924	40.2278519	37.14341354	37.6630783
47	M.BHARGAVI	46.3928833	42.5735664	46.37150955	42.7932053
48	G.PAVAN	41.30692291	39.4667625	53.89351273	45.7739983
49	HANUMANTH RAO	45.13056564	39.9531975	50.63605499	44.8386993
50	ARCHIT REDDY	53.49840546	40.0043831	58.26893997	45.1803055

Tabel 5 : test_x data for training model

The below is a test_y data which consists of about 406 subjects classification of eye defects

S No	Patient	Class
1	A.RAJASHEKAR	normal
2	S.VIJAY KUMAR	normal
3	C.SHARANYA	normal
4	D.ASHWINI	normal
5	K.SHAMALA	normal
6	H.RAMACHANDER	normal
7	G.PRAVEEN KUMAR	normal
8	J.M. MALLESWARI	normal
9	K.ARCHANA	normal
10	C.JAYASREE	normal
11	V.BHAGYA LAKSHMI	normal

12	FATIMA FIRDOUS	normal
13	MD.SAMERUDDIN	normal
14	N.RITESH RAJ	normal
15	B.SHAILAJA	normal
16	FARHEEN BEGUM	normal
17	M.SAVITHA	normal
18	MAIMUNNNISSA BEGUM	normal
19	K.PADMA	normal
20	N.MANOGNA	normal
21	K.BHAGYAVATHI	normal
22	C.PEEYUSHA	normal
23	T.SUGUNA	normal
24	M.ANWAR HUSSAIN	normal
25	MD.AYUB	normal
26	V.JAYA	normal
27	A.SURENDER	normal
28	MAHEEN	normal
29	K.JYOTHI	normal
30	BAHADOOR HANDER SINGH	normal
31	SY.MD.DILAWAR KHAN	normal
32	MD.FARIDUDDIN	normal
33	S.BALAMANI	normal

34	B.BHAVANI	normal
35	FARANA SULTHANA	normal
36	E.YELLAIAH	normal
37	T.ALIVELU	normal
38	E.S.NARENDER SWAROOP	normal
39	B.RAJ KUMAR	normal
40	G.MANISHWAR	normal
41	P.ANJAIAH	normal
42	SHAIK SARABEE	normal
43	D.GAYATHRI	normal
44	MOUNIKA	normal
45	NAYEEMA BEGUM	normal
46	A.LAXMI NARASIMHA	normal
47	M.BHARGAVI	normal
48	G.PAVAN	normal
49	HANUMANTH RAO	normal
50	ARCHIT REDDY	normal

Tabel 6 : test_y data for training model

The below is a train_x data which consists of about 105

S.No	Patient	WS_LE_radius	S_LE_radius	WS_RE_radius	S_RE_radius
1	A.RAJASHEKAR	51.8319969	42.4374504	42.6675186	43.416687
2	G.PADMA	31.7690487	28.8192635	31.8199043	29.1119709
3	BALAMANI	51.9086723	33.3805542	48.5078316	30.0094051
4	G.NAGARAJU	48.0992127	40.3113861	43.0471611	37.7262306
5	P.BHASKAR	69.0577698	54.0161934	61.1960983	46.0381889
6	G.HARSHIT SAI VENKATA CHARY	69.0470734	47.8775482	72.9401398	54.7235451
7	C.KRISHNAVENI	52.47155	33.6378975	45.4923821	35.3590431
8	P.JAMUNA	57.0046463	39.4621925	55.168232	42.0182343
9	C.OMPRAKASH	51.703579	39.4667473	50.3588142	39.8811722
10	K.RAMYA SREE	60.1041756	50.142395	58.5450401	51.2439499
11	S.DAVID	30.339922	27.7951469	29.7551422	30.1083984
12	B.PUSHPA	40.3113861	34.3293877	49.1554642	40.7002449
13	B.OMESHA MURTHY	65.7217407	63.5427971	67.22155	54.0087166
14	MD.HAMMED	41.2826614	41.512146	43.6836205	41.512146
15	k.balakrishna	46.7898827	30.1042576	46.7517738	25.7100201
16	B.AMINA	50.636055	43.5597343	57.4835129	51.7060661
17	AZMATH BEGUM	38.7203751	30.9072189	42.5500755	33.3055039
18	MD WAJIDA BEGUM	33.1476555	28.2843704	42.3586884	28.2578411
19	SHAIK MOIN	60.6736565	46.3924942	44.453167	48.6750984
20	L.JAGRUTHI	64.0664673	49.61203	72.4656067	62.0694542
21	R.STELLA MARY	46.0798492	41.8629723	59.9730377	37.7835884
22	RAJINI	44.902771	42.0090942	56.8364105	42.3086586

23	D.VENKATA SWAMY	52.4619904	39.3860092	46.1980438	39.9531975
24	A.VENKATAIAH	36.0178604	27.862896	39.3523216	32.4041786
25	MAMATHA	44.3453789	31.4170647	42.8515854	31.293663
26	S.RAJA MANI	60.5194969	42.9215393	56.3148994	47.71278
27	D.SANTHOSHI	40.4475975	35.1782646	48.9337273	33.4552918
28	N.SATHWIK	76.6262589	52.5381813	77.8606949	57.9596405
29	GOUSIA BEGUM	32.8140373	29.5170441	31.7530518	31.2011166
30	L.SATHWIK	70.7245789	63.2685356	84.258667	74.3186722
31	MD IQBAL	41.6924248	38.1183357	40.8200264	35.0216179
32	J.KEERTHI SAI	63.1052094	49.5001373	63.3465157	54.9478035
33	S.GEETANJALI	60.6508293	40.527935	44.0295067	42.3586884
34	K.BHANU PRAKASH	77.6532974	62.0186691	76.5278702	54.6146736
35	P.SUDHARSHAN	55.5023499	41.9802551	45.5028458	37.9147606
36	G.VENAKAMMA	40.8718491	33.5411186	43.2120018	36.8316231
37	MD BHASIR BHANU	45.5862312	37.6367531	50.8552856	43.7334747
38	0__AMRIN SULTHANA	51.9062653	43.4915314	39.1312904	28.4488201
39	0__V.SARASWATHI	72.993248	73.5681229	52.5818863	33.4097939
40	4__T.ANJANADEVI	64.3294144	35.9508934	61.0943718	37.9905701
41	4__MD.NASEER	37.4971085	27.7894859	36.1387215	26.1634426
42	0__N.KUNDnbai	37.6215477	28.6357422	34.0090485	27.5593147

43	4__D.ANIL KUMAR	33.5932541	27.7265072	35.0576401	30.3192349
44	0__J.YADHAIAH	36.4178162	34.0772171	36.4178162	29.9208279
45	4__S.PREMALATHA	37.0743485	30.0084305	34.6195831	25.331768
46	0__P.MUTHYALU	38.7331581	32.4732781	38.4841881	32.2847672
47	4__B.VIJAYA	45.9189453	42.3586884	48.1690712	36.8547897
48	4__SRI RAM YADAGIRI	31.8944569	28.9353714	37.2408943	36.4178162
49	0__EG.HANNAMMA	41.0214996	29.3515263	30.6621208	33.7418098
50	0__SHAHZADA BEGUM	40.3966103	27.37253	35.0464973	29.3560028

The below is a train_y data which consists of about 105 subjects classification of eye defects

S.No	Patient	Class
1	A.RAJASHEKAR	normal
2	G.PADMA	normal
3	BALAMANI	normal
4	G.NAGARAJU	normal
5	P.BHASKAR	normal
6	G.HARSHIT SAI VENKATA CHARY	normal
7	C.KRISHNAVENI	normal
8	P.JAMUNA	normal
9	C.OMPRAKASH	normal
10	K.RAMYA SREE	normal
11	S.DAVID	normal

12	B.PUSHPA	normal
13	B.OMESHA MURTHY	normal
14	MD.HAMMED	normal
15	k.balakrishna	normal
16	B.AMINA	normal
17	AZMATH BEGUM	normal
18	MD WAJIDA BEGUM	normal
19	SHAIK MOIN	normal
20	L.JAGRUTHI	normal
21	R.STELLA MARY	normal
22	RAJINI	normal
23	D.VENKATA SWAMY	normal
24	A.VENKATAIAH	normal
25	MAMATHA	normal
26	S.RAJA MANI	normal
27	D.SANTHOSHI	normal
28	N.SATHWIK	normal
29	GOUSIA BEGUM	normal
30	L.SATHWIK	normal
31	MD IQBAL	normal
32	J.KEERTHI SAI	normal
33	S.GEETANJALI	normal
34	K.BHANU PRAKASH	normal

35	P.SUDHARSHAN	normal
36	G.VENAKAMMA	normal
37	MD BHASIR BHANU	normal
38	0__AMRIN SULTHANA	cataract
39	0__V.SARASWATHI	cataract
40	4__T.ANJANADEVI	cataract
41	4__MD.NASEER	cataract
42	0__N.KUNDnbai	cataract
43	4__D.ANIL KUMAR	cataract
44	0__J.YADHAIAH	cataract
45	4__S.PREMALATHA	cataract
46	0__P.MUTHYALU	cataract
47	4__B.VIJAYA	cataract
48	4__SRI RAM YADAGIRI	cataract
49	0__EG.HANNAMMA	cataract
50	0__SHAHZADA BEGUM	cataract

CHAPTER 5

RESULTS AND DISCUSSIONS

5.1 Results

5.1.1 Feature extraction result

5.1.1.1 Calculation of pupil radius

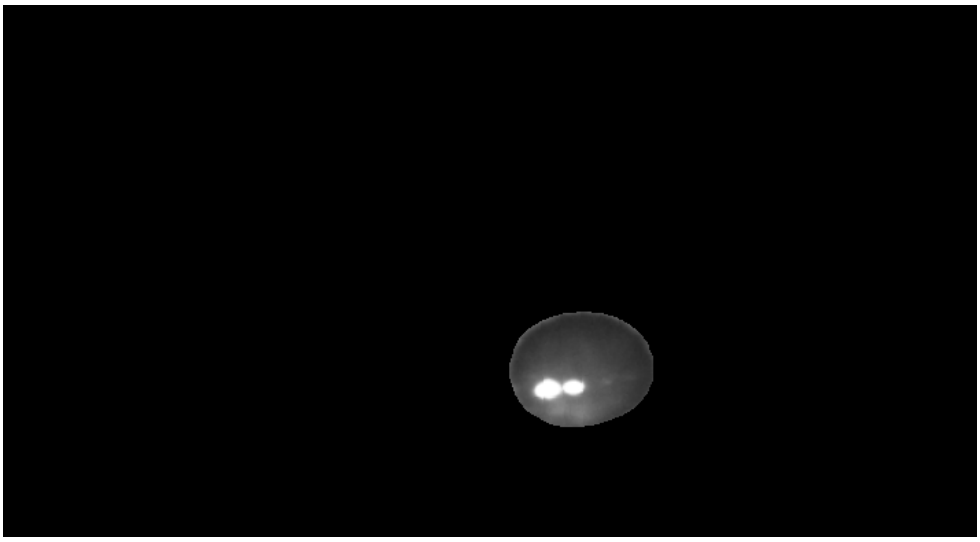

WS_RE_image:52.621620178222656

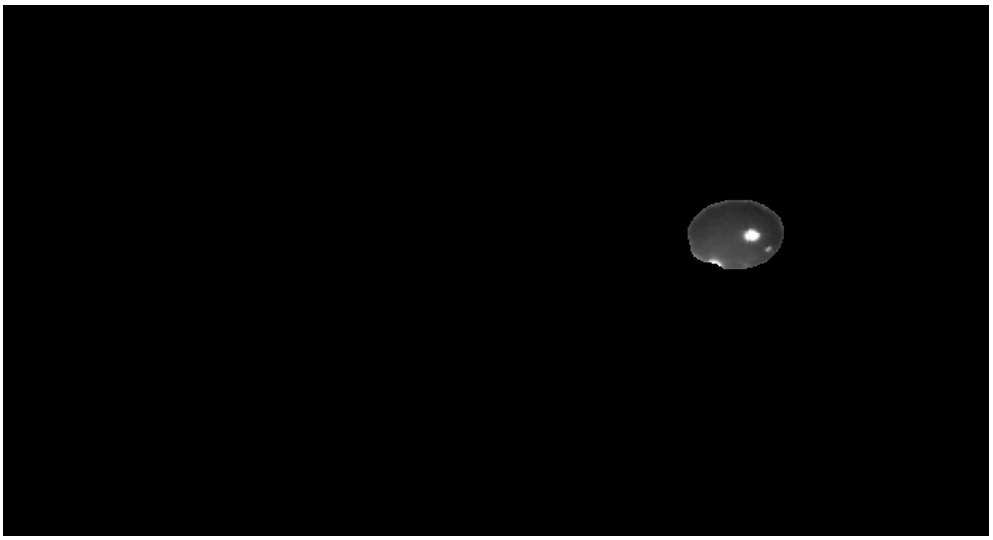

S_RE_image:33.900047302246094

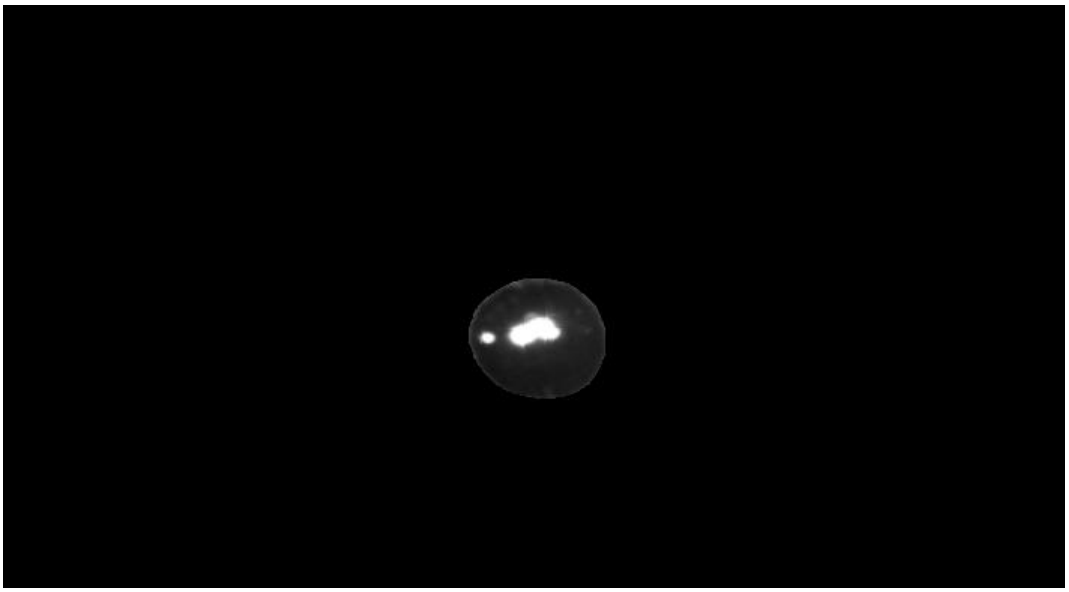

WS_LE_image:45.991947174072266

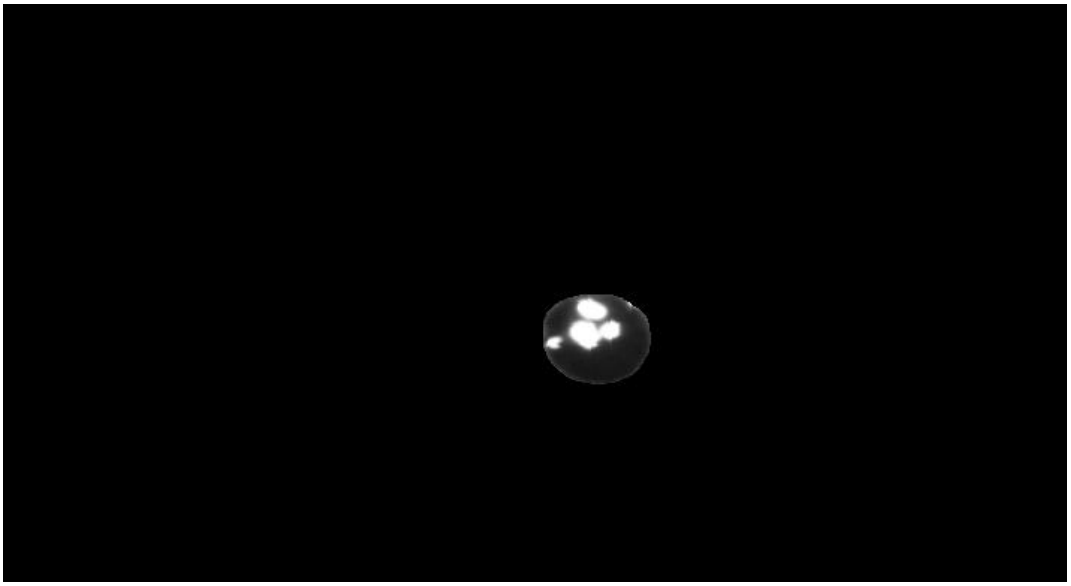

S_LE_image:36.54117202758789

5.1.2 Confusion matrix

A confusion matrix is a table that is used to evaluate the performance of a classification model or classifier. It provides a detailed breakdown of the model's predictions and the actual classes of the samples.

In the context of classifiers in deep learning, a confusion matrix is typically used for binary classification problems, where there are two classes: positive and negative. The matrix is structured as follows:

The elements of the confusion matrix represent the counts or frequencies of the model's predictions and the actual classes. Here's a breakdown of the terms used in the confusion matrix:

- True Positive (TP): The number of positive samples that are correctly classified as positive by the model.
- False Negative (FN): The number of positive samples that are incorrectly classified as negative by the model.
- False Positive (FP): The number of negative samples that are incorrectly classified as positive by the model.
- True Negative (TN): The number of negative samples that are correctly classified as negative by the model.

By examining the values in the confusion matrix, we can assess the performance of the classifier. For instance, we can calculate metrics such as accuracy, precision, recall (or sensitivity), specificity, and F1 score using the values from the confusion matrix. These metrics provide insights into the classifier's performance in terms of correctly and incorrectly classified samples. The confusion matrix helps in understanding the types of errors made by the classifier and provides a more detailed assessment of its performance than a single accuracy value. It is a valuable tool for evaluating the performance of classifiers in deep learning and making informed decisions about model improvements or adjustments

5.1.2.1 Confusion matrix of trained data

The train dataset consists of about 406 subjects data. Each subject has 4 images that are left and right eye with and without stimulus. Overall, the dataset given is 1624.

- The above is the confusion matrix obtained after training the data. The results obtained are as follows: The model is given with 144 normal eye dataset obtain from subjects and it is trained that with 100 percent accuracy such that the true labels are equal to predicted labels.
- Similarly the 128 catract and 134 blurred eye dataset is given to train the model with 100 percent accuracy such that the true labels are equal to predicted labels.

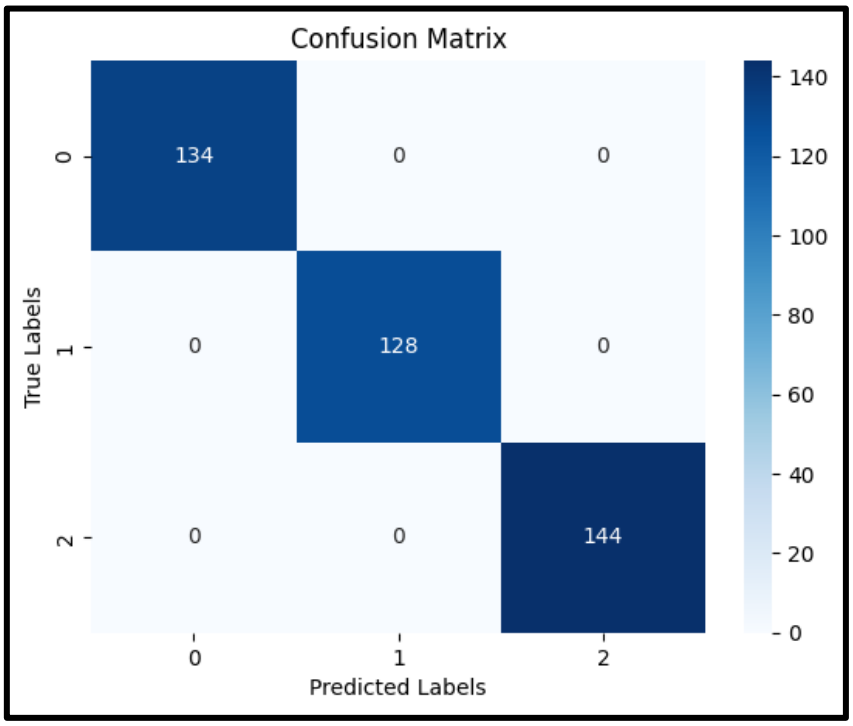

Fig: 5.1.confusion matrix of trained data

5.1.2.2 Confusion matrix of tested data

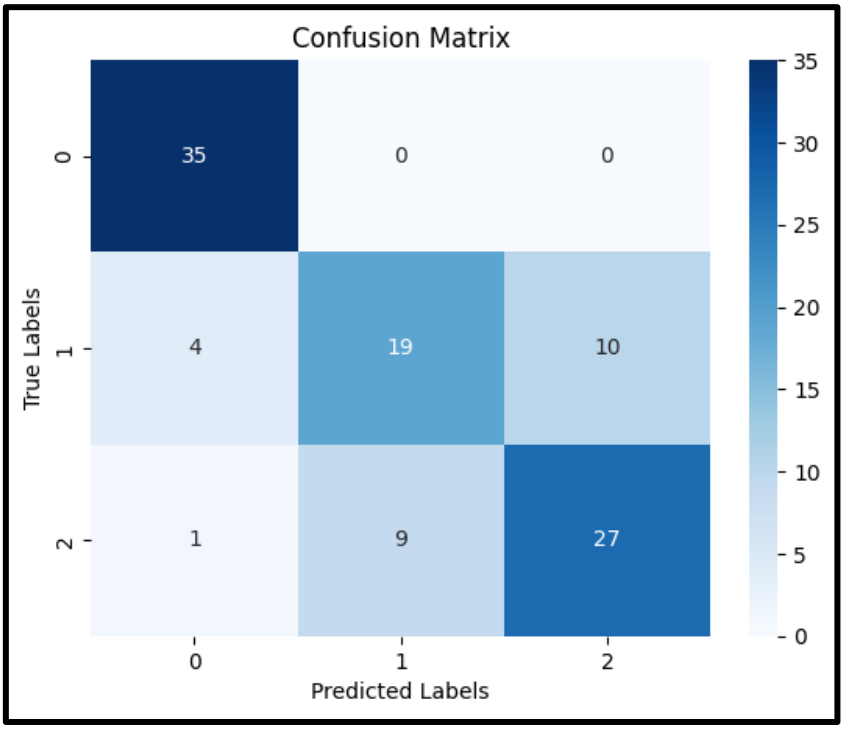

Fig: 5.2.confusion matrix of tested data

The test dataset consists of about 105 subjects data. Each subject has 4 images that are left and right eye with and without stimulus. Overall, the dataset given is 420.

The above is the confusion matrix obtained after testing the data. The results obtained are as follows:

- The model is given with 37 normal eye dataset obtain from subjects and it has predicted that among 37, 27 as normal, 9 as the cataract and 1 as blurred with 88 percent accuracy.
- Similarly the model is given with 33 cataract dataset obtain from subjects and it has predicted that among 33, 10 as normal, 19 as the cataract and 4 as blurred with 89 percent accuracy.
- Model is given with 35 blurred dataset obtain from subjects and it has predicted that among 35, 35 blurred with 100 percent accuracy.

5.1.3. ROC Curve

ROC stands for Receiver Operating Characteristic. In the context of classifiers in deep learning, ROC is a graphical representation of the performance of a binary classifier as the discrimination threshold is varied. It is commonly used to evaluate and compare the performance of classifiers in terms of their ability to correctly classify positive and negative samples.

The ROC curve is created by plotting the True Positive Rate (TPR) against the False Positive Rate (FPR) at various threshold settings. The TPR, also known as sensitivity or recall, represents the proportion of positive samples correctly classified as positive. The FPR, on the other hand, represents the proportion of negative samples incorrectly classified as positive. The TPR is plotted on the y-axis, and the FPR is plotted on the x-axis.

A perfect classifier would have a TPR of 1 and an FPR of 0, resulting in a point at the top-left corner of the ROC curve. As the discrimination threshold is changed, the classifier's performance may vary, and different points on the ROC curve are obtained. The closer the curve is to the top-left corner, the better the classifier's performance, indicating a higher TPR and a lower FPR.

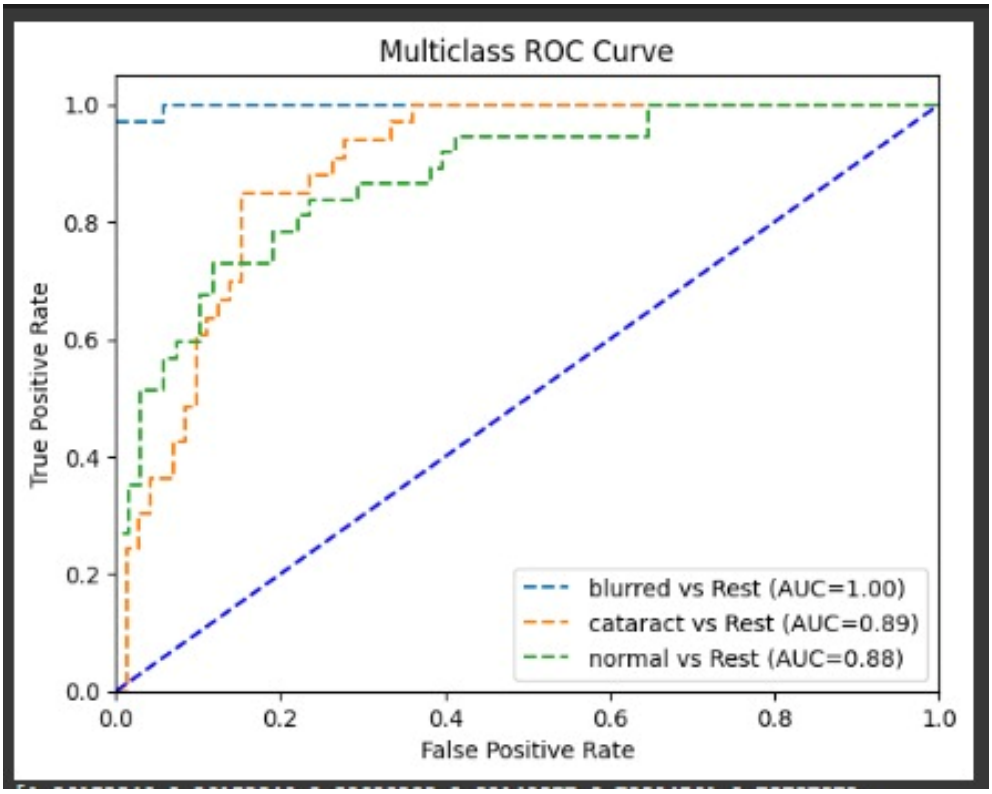

Fig. 5.3 ROC curve

The Roc curve obtained from the tested data is shown above. The blue line would predic that the model is 50% accurate and if the curve is above blue is considered as accurate and below is considered to be less accurate accordingly.

On testing the data the accuracy produced for blurred, cataract and normal as 1.00,0.89 and 0.88.

Model is considered as accurate if the curve has accuracy of 1.00.

The overall accuracy of model in detecting the normal,cataract and blurred visions is 77.14 percent.

5.1.4. Precision-recall curve

A precision-recall curve is a graphical representation of the trade-off between precision and recall for a binary classification model. It is commonly used to evaluate the performance of models, especially in situations where the data is imbalanced or the cost of false positives and false negatives is different.

Precision is the ratio of true positives to the sum of true positives and false positives. It represents the accuracy of the positive predictions made by the model. Precision measures

how well the model correctly identifies positive instances out of all instances it predicts as positive.

Recall, also known as sensitivity or true positive rate, is the ratio of true positives to the sum of true positives and false negatives. It represents the proportion of actual positive instances that the model correctly identifies. Recall measures how well the model captures all positive instances in the dataset.

The precision-recall curve visualizes the relationship between precision and recall as the classification threshold or decision boundary of the model varies. It is created by calculating precision and recall values at different threshold levels. Each point on the curve represents a specific threshold, and the curve shows how precision and recall change as the threshold is adjusted.

The precision-recall curve is useful for evaluating the performance of a model in scenarios where the class distribution is imbalanced or when there is a need to prioritize either precision or recall based on the specific requirements of the problem. It provides insights into how different threshold levels impact the trade-off between precision and recall and helps in selecting an appropriate threshold for the desired balance between the two metrics.

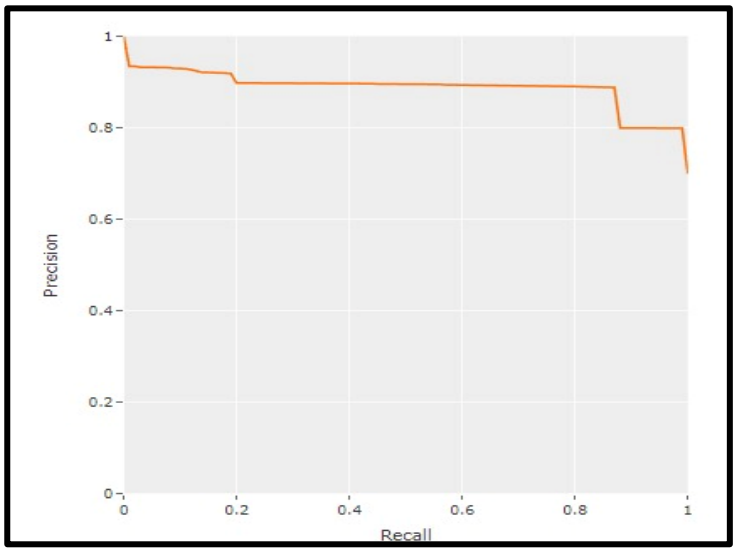

Fig. 5.4 Precision graph

5.1.5. Accuracy, Precision, recall and F1 score

5.1.5.1 Accuracy

Accuracy score is a commonly used metric to evaluate the performance of a classification model in deep learning. It measures the percentage of correctly classified samples out of the total number of samples.

The accuracy score provides an overall measure of how well the classifier is able to correctly predict the class labels of the samples. A higher accuracy score indicates a better performance, as it indicates a higher proportion of correctly classified samples.

However, it is important to note that accuracy score may not always be the most suitable metric, especially in cases where the classes are imbalanced or when the cost of misclassification differs for different classes. In such scenarios, other metrics such as precision, recall, F1 score, or area under the ROC curve (AUC-ROC) may provide a more comprehensive evaluation of the classifier's performance.

It is recommended to consider multiple metrics and analyze the confusion matrix to gain a better understanding of the classifier's strengths and weaknesses. Evaluating the accuracy score alongside other relevant metrics can help assess the overall performance of the deep learning classifier.

The accuracy obtained from after testing the model is 77.14 percent.

```
[ ]  from sklearn.metrics import accuracy_score

     acc = accuracy_score(y_test, y_pred)
     print('accuracy_score: ', acc)

     accuracy_score:  0.7714285714285715

[ ]  from sklearn.metrics import classification_report

     report = classification_report(y_test, y_pred)

     print(report)

                   precision    recall  f1-score   support

                0       0.87      0.97      0.92        35
                1       0.69      0.61      0.65        33
                2       0.73      0.73      0.73        37

         accuracy                           0.77       105
        macro avg       0.76      0.77      0.76       105
     weighted avg       0.76      0.77      0.77       105
```

Fig. 5.5 Classification report

5.1.5.2 Precision

Precision is a metric used to evaluate the performance of a classification model in deep learning. It measures the proportion of correctly predicted positive samples out of the total number of samples predicted as positive. Precision focuses on the accuracy of positive predictions.

In the context of deep learning classifiers, precision is calculated as:

Precision = TP / (TP + FP)

where TP represents the number of true positive samples (correctly predicted positive) and FP represents the number of false positive samples (negative samples incorrectly predicted as positive).

Precision helps assess the classifier's ability to avoid false positive predictions. A high precision value indicates that the classifier has a low rate of falsely labeling negative samples as positive. It shows the model's capability to accurately identify positive samples and minimize false positive errors.

Precision is particularly useful in situations where false positives are costly or have significant consequences. For example, in medical diagnosis, precision is important to minimize the number of false positive predictions for a disease.

The precision obtained for blurred(0), cataract(1) and normal(2) is 0.87 ,0.69 and 0.73 respectively.

5.1.5.3 Recall

Recall, also known as sensitivity or true positive rate (TPR), is a metric used to evaluate the performance of a classification model in deep learning. It measures the proportion of correctly predicted positive samples out of the total number of actual positive samples. Recall focuses on the ability of the model to correctly identify positive samples.

In the context of deep learning classifiers, recall is calculated as:

Recall = TP / (TP + FN)

where TP represents the number of true positive samples (correctly predicted positive) and FN represents the number of false negative samples (positive samples incorrectly predicted as negative).

Recall helps assess the classifier's ability to correctly identify positive samples and avoid false negatives. A high recall value indicates that the classifier has a low rate of falsely labeling positive samples as negative. It shows the model's capability to capture a high proportion of positive samples in the dataset.

Recall is particularly important in scenarios where false negatives are costly or have significant consequences. For example, in medical diagnosis, it is crucial to minimize the number of false negative predictions for a disease to avoid missing important cases.

The recall obtained for blurred(0), cataract(1) and normal(2) is 0.97 ,0.61 and 0.73 respectively.

5.1.5.4 F1 score

The F1 score is a metric used to evaluate the performance of a classification model in deep learning. It combines both precision and recall into a single value and provides a balanced measure of a model's accuracy.

In the context of deep learning classifiers, the F1 score is calculated as the harmonic mean of precision and recall:

F1 Score = 2 * (Precision * Recall) / (Precision + Recall)

The F1 score ranges from 0 to 1, where a higher value indicates better performance. It takes into account both false positives (precision) and false negatives (recall) and provides a balanced assessment of the classifier's ability to correctly classify both positive and negative samples.

The F1 score is particularly useful in situations where there is an imbalance between the classes or when false positives and false negatives have different implications. It provides a single metric that considers both precision and recall, allowing for a comprehensive evaluation of the classifier's performance.

When the precision and recall values are both high, the F1 score will be close to 1, indicating a well-performing classifier. On the other hand, if either precision or recall is low, the F1 score will also be low, highlighting areas where the classifier needs improvement.

The F1 score is commonly used in deep learning and other classification tasks as a measure of overall accuracy, considering both precision and recall simultaneously.

The F1 score obtained for blurred(0), cataract(1) and normal(2) is 0.92 ,0.65 and 0.73 respectively.

CHAPTER 6

CONCLUSION

6.1 Conclusion

Relative afferent pupillary defect is a serious ocular disease and the number of people affected by this disease is increasing over the years. Design and development of pupillometer has been done for detection of RAPD and eye defects with following results:

- The pupil and its radius is detected and accuracy obtained was 90.5 percent
- The proposed novel device is able to classify the images as cataract, blurry vision, and normal based on the tested data with accuracy of 77.14 percent.
- The precision obtained for blurred (0), cataract (1) and normal (2) is 0.87 ,0.69 and 0.73 respectively.
- The recall obtained for blurred (0), cataract (1) and normal (2) is 0.97 ,0.61 and 0.73 respectively.
- The F1 score obtained for blurred (0), cataract (1) and normal (2) is 0.92 ,0.65 and 0.73 respectively.

6.2 Future work

The prospects of the current project are vast. In this thesis we have presented a pupillometer device for the detection of RAPD, cataract and blurred vision using deep learning by acquiring the images under the stimulus and non-stimulus condition. Further, the work can be extended by simultaneously making the pupillometer automated for real time acquisition and measuring the pupil radius and accordingly classifying whether the person suffering from eye defects.

REFERENCES

[1] Clinical Anatomy of the Eye; Second Edition – Richard S. Snell, Michael A. Lemp

[2] Clinical Anatomy of the Visual System; Second Edition – LEE ANN REMINGTON

[3] Jack J Kanski Clinical Ophthalmology; Sixth Edition

[4] Bell, Raymond A., et al. "Clinical grading of relative afferent pupillary defects." *Archives of Ophthalmology* 111.7 (1993): 938-942

[5] http://www.richmondeye.com/clinical-content-the-relative-afferentpupillary-defect/

[6] Thompson, H. Stanley, and James J. Corbett. "Asymmetry of pupillomotor input." *Eye* 5.Pt 1 (1991): 36-9

[7] Cox, Terry A. "Pupillary escape." *Neurology* 42.7 (1992): 1271-1271.

[8] Enyedi, Laura B., Sundeep Dev, and Terry A. Cox. "A comparison of the Marcus Gunn and alternating light tests for afferent pupillary defects. *"Ophthalmology* 105.5 (1998): 871-873.

[9] v, Graefe, A.; Mitteilungen vermischten Inhalts: 12: Ueber ein einfaches Mittel, Simulation einseitiger Amaurose zu entdecken, nebst Bemerkungen ueber die Pupillar-Kontraction b^i Erblindeten. Arch. f. Ophth. 2:266 (pt. 1) 1855

[10] Gerold, Hugo. *Die Lehre vom schwarzen Staar u. dessen Heilung*. Rubach, 1846

[11] Hirschberg, J. "Neuritis retrobulbaris." *Z. Prak. Augenh* 8 (1884): 185. [12] Baquis, E. "La reazione pupillare come elemento diagnostico differenziale tra l'amaurosi isterica e quella da nevrite retro-bulbare." *Ann. Ottal* 30.3 (1901): i901

[13] Gunn, R. Marcus, et al. "Discussion on retro-ocular neuritis." *The British Medical Journal* (1904): 1285-1287.

[14] Kestenbaum, Alfred. *Clinical methods of neuro-ophthalmologic examination*. Elsevier, 2013.

[15] LEVATIN, PAUL. "Pupillary escape in disease of the retina or optic nerve."*AMA Archives of Ophthalmology* 62.5 (1959): 768-779

[16] Thompson, H. Stanley. "Afferent pupillary defects: Pupillary findings associated

with defects of the afferent arm of the pupillary light reflex arc."*American journal of ophthalmology* 62.5 (1966): 860-873

[17]Thompson, H. St. "Pupillary signs in the diagnosis of optic nerve disease."*Transactions of the ophthalmological societies of the United Kingdom* 96.3 (1976): 377

[18] Digre, K. B. "Principles and techniques of examination of the pupils, accommodation, and the lacrimal system." *Walsh & Hoyt's clinical neuroophthalmology* 1 (1998): 933-1040

[19] Thompson, H. Stanley, James J. Corbett, and Terry A. Cox. "How to measure the relative afferent pupillary defect." *Survey of ophthalmology* 26.1 (1981): 39-42

[20] Arnold, Robert W. "Quantification of afferent pupillary defect by double polarized filter." *Archives of ophthalmology* 108.12 (1990): 1666-1667

[21] Rosenberg, Michael L., and Armando Oliva. "The use of crossed polarized filters in the measurement of the relative afferent pupillary defect." *American journal of ophthalmology* 110.1 (1990): 62-65

[22] Ramsay, Andrew, et al. "Crossed polarising filters to measure relative afferent pupillary defects: reproducibility, correlation with neutral density filters and use in central retinal vein occlusion." *Eye* 9.5 (1995): 624-628

[23] McCormick, A., et al. "Quantifying relative afferent pupillary defects using a Sbisa bar." *British journal of ophthalmology* 86.9 (2002): 985-987

[24] Bremner, F. D. "Pupil assessment in optic nerve disorders." *Eye* 18.11 (2004): 1175-1181

[25] Kawasaki, Aki, Paula Moore, and Randy H. Kardon. "Long-term fluctuation of relative afferent pupillary defect in subjects with normal visual function."*American journal of ophthalmology* 122.6 (1996): 875-882

[26] Lam, Byron L., and H. Stanley Thompson. "An anisocoria produces a small relative afferent pupillary defect in the eye with the smaller pupil." *Journal of neuroophthalmology* 19.3 (1999): 153-159

[27] Lam, Byron L., and H. Stanley Thompson. "A unilateral cataract produces a relative afferent pupillary defect in the contralateral eye." *Ophthalmology*97.3 (1990): 334-338

[28] Stern, H. J. "A simple method for the early diagnosis of abnormalities of the pupillary reaction." *The British journal of ophthalmology* 28.6 (1944): 275 [29] Miller, Stephen

D., and H. Stanley Thompson. "Edge-light pupil cycle time."*British Journal of Ophthalmology* 62.7 (1978): 495-500

[30]Miller, Stephen D., and H. Stanley Thompson. "Pupil cycle time in optic neuritis." *American journal of ophthalmology* 85.5 Pt 1 (1978): 635-642

[31] Hamilton, W., and R. D. Drewry Jr. "Edge-light pupil cycle time and optic nerve disease." *Annals of ophthalmology* 15.8 (1983): 714-721

[32] Kirkham, T. H., and S. G. Coupland. "Multiple regression analysis of diagnostic predictors in optic nerve disease." *Canadian Journal of Neurological Sciences/Journal Canadien des Sciences Neurologiques* 8.01 (1981): 67-72 [33] Manor, R. S., Y. Yassur, and I. Ben-Sira. "Pupil cycle time in noncompressive optic neuropathy." *Annals of ophthalmology* 14.6 (1982): 546-550

[34] Weinstein, J. M., J. C. Van Gilder, and H. S. Thompson. "Pupil cycle time in optic nerve compression." *American journal of ophthalmology* 89.2 (1980): 263-267 [35] Manor, R. S., Y. Yassur, and Sira I. Ben. "Pupil cycle time in space occupying lesions of anterior optic pathways." *Annals of ophthalmology*14.11 (1982): 1030-1031 [36] Wilhelm, Helmut, et al. "The prevalence of relative afferent pupillary defects in normal subjects." *Journal of Neuro-Ophthalmology* 27.4 (2007): 263-267

[37] Radzius, Aleksandras, et al. "A portable pupilometer system for measuring pupillary size and light reflex." *Behavior Research Methods, Instruments, & Computers* 21.6 (1989): 611-618

[38] Kalaboukhova, Lada, Vanja Fridhammar, and Bertil Lindblom. "An objective method for measuring relative afferent pupillary defect in glaucomatous optic neuropathy—stimulus optimization." *Neuro-ophthalmology* 30.1 (2006): 7-15 [39] Miki, Atsushi, et al. "Pupillography of relative afferent pupillary defect contralateral to monocular mature cataract." *Canadian Journal of Ophthalmology/Journal Canadien d'Ophtalmologie* 41.4 (2006): 469-471

[40] Miki, Atsushi, et al. "Pupillography of relative afferent pupillary defects in amblyopia associated with peripapillary myelinated nerve fibres and myopia."*Journal of pediatric ophthalmology and strabismus* 45.5 (2008): 309-312

[41] Cohen, Liza M., et al. "A novel computerized portable pupillometer detects and quantifies relative afferent pupillary defects." *Current eye research* 40.11 (2015): 1120-1127

[42] Volpe, Nicholas J., et al. "Portable pupillography of the swinging flashlight test to detect afferent pupillary defects." *Ophthalmology* 107.10 (2000): 1913-1921 [43]Cox, Terry A. "Pupillographic characteristics of simulated relative afferent pupillary defects." *Investigative ophthalmology & visual science* 30.6 (1989): 1127-
1131

[44] Volpe, Nicholas J., et al. "Computerized binocular pupillography of the swinging flashlight test detects afferent pupillary defects." *Current eye research* 34.7 (2009): 606-613

[45] Miki, Atsushi, et al. "Pupillography of automated swinging flashlight test in amblyopia." *Clinical ophthalmology (Auckland, NZ)* 2.4 (2008): 781

[46] Dara Lankaranian, M. D., and George L. Spaeth. "The usefulness of a new method of testing for a relative afferent pupillary defect in patients with ocular hypertension and glaucoma." *Trans Am Ophthalmol Soc* 103 (2005): 200-208 [47] Benson, M. T., et al. "A novel approach to the assessment of afferent pupillary defects." *Eye* 5.Pt 1 (1991): 40-44

[48] Shwe-Tin, Audrey, et al. "Evaluation and calibration of a binocular infrared pupillometer for measuring relative afferent pupillary defect." *Journal of Neuro-Ophthalmology* 32.2 (2012): 111-115